# Do vacuum fluctuations prevent the creation of closed timelike curves?

Sung-Won Kim* and Kip S. Thorne

*Theoretical Astrophysics, California Institute of Technology, Pasadena, California 91125*

(Received 12 September 1990; revised manuscript received 5 March 1991)

It has been shown elsewhere that in a classical spacetime with multiply connected space slices (wormhole spacetime), closed timelike curves can form generically. The boundary between an initial region of spacetime without closed timelike curves and a later region with them is a Cauchy horizon which can be stable against small classical perturbations. This paper investigates stability against vacuum fluctuations of a quantized field, by calculating the field's renormalized stress-energy tensor near the Cauchy horizon. The calculation is restricted to a massless, conformally coupled scalar field, but it is argued that the results will be the same to within factors of order unity for other noninteracting quantum fields. The calculation is given in order of magnitude for any spacetime with closed timelike curves, and then a detailed calculation is given for a specific example of such a spacetime: one with a traversable wormhole whose mouths create closed timelike curves by their relative motions. The renormalized stress-energy tensor is found to diverge as one approaches the Cauchy horizon. However, the divergence is extremely weak: so weak, that as seen in the rest frame of one of the wormhole mouths the vacuum polarization's gravity distorts the spacetime metric near the mouth by only $\delta g_{\mu\nu}^{\rm VP} \sim (l_P/D)(l_P/\Delta t)$, where $\Delta t$ is the proper time until one reaches the Cauchy horizon and $D$ is the distance between the two mouths when the Cauchy horizon forms. For a macroscopic wormhole with $D \sim 1$ m, $\delta g_{\mu\nu}^{\rm VP}$ has only grown to $l_P/D \sim 10^{-35}$ when one is within a Planck length of the horizon. Since the very concept of classical spacetime is normally thought to fail, and be replaced by the quantum foam of quantum gravity on scales $\Delta t \lesssim l_P$, the authors are led to conjecture that the vacuum-polarization divergence gets cut off by quantum gravity upon reaching the tiny size $l_P/D$, and spacetime remains macroscopically smooth and classical and develops closed timelike curves without difficulty. Hawking, in response to this, has conjectured that the spacetime near the Cauchy horizon remains classical until $D\Delta t$ (which in a certain sense is frame invariant) gets as small as $\sim l_P^2$, and correspondingly until $\delta g_{\mu\nu}^{\rm VP} \sim 1$, and that, as a result, the vacuum-polarization divergence will prevent the formation of closed timelike curves. These two conjectures are discussed and contrasted. The attempt to test them might produce insight into candidate theories of quantum gravity.

## I. INTRODUCTION AND SUMMARY

It may be that the laws of semiclassical gravity (general relativity plus quantum field theory in curved spacetime) permit the existence of classical, traversable wormholes (topological handles in space through which timelike and null curves can pass).[1,2,3] If so, then classical general relativity predicts that generic relative motions of a wormhole's mouths and/or generic externally produced gravitational redshifts will dynamically change the manner in which time connects up through the wormhole, thereby creating closed timelike curves (CTC's) that loop through the wormhole.[2,4]

In this situation (and any other where initially spacetime is asymptotically flat and devoid of CTC's, and later CTC's arise), the boundary between the early region of spacetime without CTC's and the later one with them is a Cauchy horizon.[5,2,6] If the Cauchy horizon were unstable against perturbations produced by fields that reside in the spacetime, and if the instability were sufficiently strong, then that instability might prevent the formation of CTC's.

Indeed, there *is* such an instability for some sets of wormhole parameters (e.g., a wormhole in flat spacetime whose mouths are moving toward each other at high speed and whose Cauchy horizon arises when the mouths are sufficiently close together). For such wormholes, high-frequency waves of any zero-rest-mass, *classical* field can loop through the wormhole over and over again, piling up on themselves at the Cauchy horizon. The result is a stress energy that diverges as one approaches the Cauchy horizon (at least in the test-field limit) and that, via the spacetime curvature it produces, might well destroy the horizon and prevent the creation of CTC's.[2]

This classical instability is counteracted by the wormhole's "diverging-lens" action: The wormhole drives the waves' amplitude down, with each circuit, by a factor $b/2D$, where $b$ is the radius of the wormhole throat and $D$ is the distance between the wormhole mouths when the Cauchy horizon arises. If $D$ is sufficiently large, this attenuation prevents the field's classical stress energy from diverging at the Cauchy horizon; there is no instability; and the classical field thus is unable to prevent creation of CTC's.[2,7]

Those of us who have been studying these issues suspected, at first, that this same diverging-lens action would also stabilize the Cauchy horizon against the vacuum fluctuations of quantum fields. However, closer scrutiny quickly disspelled this misconception: In unpublished work, a number of people[8] independently discovered that, at any event in spacetime which can be joined to itself by a closed null geodesic (CNG), the vacuum fluctuations of a massless scalar field should produce a divergent renormalized stress-energy tensor (divergent vacuum polarization). Since every event on a Cauchy horizon at which CTC's arise is arbitrarily close to the identical end points of a CNG (cf. Secs. II A, V A, and VI A), this means that the vacuum polarization must diverge everywhere on the Cauchy horizon.

In Sec. II of this paper we derive the order-of-magnitude form of the vacuum-polarization divergence for any spacetime with CTC's, and then in Secs. V and VI we compute the full details of the divergence for a specific spacetime in which relative motion of a wormhole's two mouths produces the CTC's. Elsewhere, Frolov[9] computes the full details for locally static spacetimes in which the CTC's are produced by a difference in the gravitational redshifts at two wormhole mouths. These derivations are all confined to the idealized case of a conformally coupled, massless scalar field. However, experience with vacuum polarization in other contexts (especially the Casimir effect,[10] which is closely related to our vacuum polarization; see Sec. VI D) suggests that other quantum fields will exhibit the same behavior as our scalar field, aside from signs and numerical factors of order unity. At least this is likely to be so for noninteracting quantum fields; there are hints,[11] though not strong ones, that self-interaction might cause severe problems for physics in the presence of closed timelike curves.

Will the divergence of the vacuum polarization, at a Cauchy horizon where CTC's are trying to form, destroy the horizon and prevent the creation of the CTC's? Perhaps not. A Planck-length cutoff on the existence of classical spacetime may well prevent the vacuum stress-energy tensor from growing large enough to destroy the Cauchy horizon.

The key to the Planck-length cutoff is the fact that spacetime is classical only on length scales larger than the Planck length, $l_P \sim 10^{-33}$ cm. On length scales less than or of order $l_P$, quantum gravity fluctuations in the curvature of spacetime are so large that the concept of classical spacetime makes no sense.[12] Correspondingly, the renormalized stress-energy tensor computed using semiclassical gravity theory (quantum field theory in classical, curved spacetime) must cease to be meaningful when it is scrutinized on length scales less than or of order $l_P$; and divergences occurring on such length scales must not be believed.

Only the (as yet incomplete) theory of quantum gravity can tell us *for sure* what happens on such length scales. However, it turns out (Secs. II E, V D, V E, VI D, and VI E) that the divergence of a quantum field's

renormalized stress-energy tensor is rather weak. It is so weak in fact that, as any observer in any reference frame appropriate to the macroscopic spacetime (e.g., the rest frame of a wormhole mouth) approaches any Cauchy horizon where CTC's arise, the observer sees the spacetime curvature produced by the field's stress energy get completely swamped by the quantum fluctuations of curvature long before he gets within a Planck length of the horizon. More specifically, the vacuum-polarization-induced curvature distorts the metric by amounts $\delta g_{\mu\nu}^{\rm VP} \sim (l_P/D)(l_P/\Delta t)$ (where $D$ is the spatial length of the closed null geodesics on or near the Cauchy horizon, as seen in the observer's frame and $\Delta t$ is the time until the observer crosses the Cauchy horizon), whereas the quantum-gravity fluctuations of geometry, even in macroscopically flat spacetime, have magnitude $\delta g_{\mu\nu}^{\rm QG} \sim l_P/\Delta t \gg \delta g_{\mu\nu}^{\rm VP}$. Correspondingly, it seems reasonable to expect that the vacuum-polarization divergence will get smeared out by quantum-gravity effects.

If we approximate this smearing out by the simple artifice of terminating the divergence when the observer is within a distance $\Delta t \sim l_P$ of the Cauchy horizon, then the resulting maximum $\delta g_{\mu\nu}^{\rm VP} \sim l_P/D$ ($\sim 10^{-35}$ if $D \sim 1$ m) is so weak that it has no hope of preventing the creation of CTC's. (See Sec. II E for further detail.) This led the authors, in the originally submitted version of this paper, to conjecture vigorously that the diverging vacuum polarization will not prevent the creation of closed timelike curves.

Hawking,[13] in response to the originally submitted version of this paper, has criticized the above estimate of where quantum gravity invalidates the computed $\delta g_{\mu\nu}^{\rm VP} \sim (l_P^2/D\Delta t)$. The quantities $D$ and $\Delta t$ depend on the observer's reference frame, he points out, but the product $D\Delta t$ does not. Therefore, he conjectures, it may well be that the spacetime remains classical, near the Cauchy horizon, and the computed $\delta g_{\mu\nu}^{\rm VP}$ remains correct, until the product $D\Delta t$ gets as small as $l_P^2$, and correspondingly $\delta g_{\mu\nu}^{\rm VP}$ reaches unity. The resulting distortion of the classical spacetime geometry might then be sufficient always to prevent the creation of CTC's, Hawking speculates. He calls his speculation the "chronology protection conjecture." We have inserted into this final version of our paper a brief section (Sec. II F) that compares and contrasts Hawking's conjecture with ours. It is not at all obvious to us now which conjecture (if either) is correct.

The body of this paper is organized as follows: In Sec. II we give our order-of-magnitude computation of the effects of vacuum polarization and our discussion of Hawking's conjecture and ours. In Secs. III and IV we lay foundations for our detailed, quantitative computation of vacuum polarization: Sec. III derives a geometric-optics approximation to the Hadamard function at points in spacetime near which there are closed null geodesics, and Sec. IV computes the detailed geometric features of the specific spacetime in which our analysis is carried out. Then in Secs. V and VI we use a point-splitting regularization, based on the geometric-optics Hadamard

function of Sec. III, to compute the scalar field's renormalized stress-energy tensor $T^{\mu\nu}$. In Sec. V we evaluate $T^{\mu\nu}$ near the throat of the wormhole, and in Sec. VI we evaluate it between the two mouths and far from them.

Finally, in Sec. VII we list possible (but in our view unlikely) flaws in our analysis, and we discuss some implications of our results: If, as we conjecture (and Hawking disagrees), vacuum fluctuations are unable to prevent the creation of closed timelike curves, what can prevent their creation? Or are they, perhaps, allowed?

Throughout this paper (except in the discussion of the physical implications of our results, Sec. II E) we use "natural units," $c = G = \hbar = 1$, and we use the sign conventions of Misner, Thorne, and Wheeler.[14]

## II. ORDER-OF-MAGNITUDE ANALYSIS FOR ANY WORMHOLE SPACETIME WITH CTC'S

In this section we shall carry out an order-of-magnitude calculation of the renormalized stress-energy tensor for a conformally coupled scalar field $\phi$ in an arbitrary spacetime with closed timelike curves, and we shall discuss the physical implications of our calculation.

This section is organized as follows: In subsection A we shall introduce and explore the concept of *polarized hypersurfaces*. These are the hypersurfaces in spacetime at which the renormalized stress-energy tensor diverges (before one takes account of the effects of quantum gravity). In subsection B we shall briefly sketch the point-splitting approach to computation of the renormalized stress-energy tensor. In subsection C we shall sketch a geometric-optics approach to evaluating the Hadamard function, which underlies the point-splitting calculation. In subsection D we shall evaluate the Hadamard function, in order of magnitude, near a polarized hypersurface, and then shall use it to compute the renormalized stress-energy tensor. In subsection E we shall examine the physical consequences of our stress-energy tensor and its apparent divergence at the polarized hypersurface and also at the Cauchy horizon (which is a limit of polarized hypersurfaces), and we shall discuss our conjecture that quantum gravity smears out the divergence and permits the CTC's to form. In subsection F we shall discuss Hawking's chronology protection conjecture, and compare and contrast it with our own conjecture.

### A. Polarized hypersurfaces

Although this section deals with an arbitrary spacetime with closed timelike curves, as a conceptual aid we frequently shall refer to a specific example of such a spacetime: the example that is treated in detail in Secs. III–VI. That example is depicted in Fig. 1.

The wormhole of our example resides in flat, Minkowskii spacetime and has an infinitesimally short throat. The wormhole's left mouth (mouth 1) is at rest in the Lorentz coordinate system $(T, X, Y, Z)$ of the figure, and its right mouth (mouth 2) moves toward its left
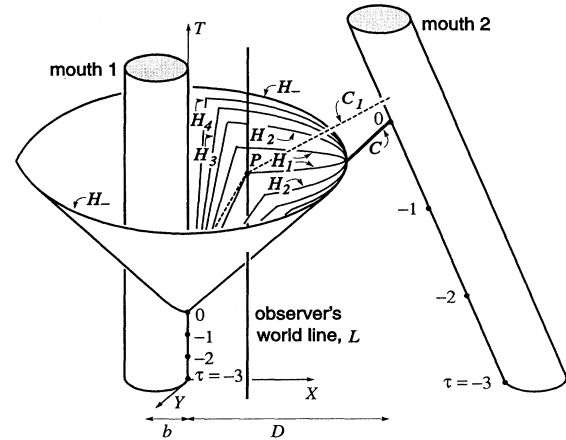


FIG. 1. The wormhole spacetime studied quantitatively in this paper.

mouth along the $X$ axis. The right edge of mouth 1 (as seen in the diagram) is the same world line as the left edge of mouth 2. (The wormhole's mouths and throat coincide because it is infinitesimally short.) Proper time $\tau$, as measured by an observer at rest on that edge of the mouths/throat, is marked off in the diagram. There is a very special closed null geodesic (CNG) $\mathcal{C}$ that starts at $\tau = 0$ on the throat, exits from mouth 1, runs along the $X$ axis from mouth 1 to mouth 2, then returns to its starting point, $\tau = 0$ on the throat, joining smoothly onto itself. This CNG is a "fountain" from which springs the Cauchy horizon $\mathcal{H}_-$: The Cauchy horizon is generated by (nonclosed) null geodesics that all asymptote to $\mathcal{C}$ when followed into the past. For a proof and detailed discussion, see the Appendix of Ref. 6.

Figure 1 shows a portion of the Cauchy horizon $\mathcal{H}_-$. It is, roughly speaking, a future light cone of the event $\tau = 0$ on the wormhole's mouth 1.

Since the renormalized stress-energy tensor diverges at events that are joined to themselves by CNG's, such events play an important role in this paper. The CNG joining any such event to itself (e.g., $\mathcal{C}_1$ in Fig. 1, which joins $\mathcal{P}$ to itself) must somewhere go backward in the Lorentz time $T$ of the external universe in order to return to its starting event; and the only way it can do this is by traversing the wormhole. Those events that are joined to themselves by CNG's which traverse the wormhole precisely $N$ times form a hypersurface in spacetime that we shall denote $\mathcal{H}_N$, and shall call the "$N$th polarized hypersurface." (This name refers to the fact that the vacuum polarization diverges at such a hypersurface, and also to the fact that the structure of the divergent vacuum polarization is somewhat like that of a layer of dipoles, as we shall see in Sec. II E.)

The locations of the polarized hypersurfaces $\mathcal{H}_1$, $\mathcal{H}_2$,

$\mathcal{H}_3, \ldots$ are computed, in the vicinity of $\mathcal{C}$, in Secs. V A and VI A, and are depicted in Fig. 1. These $\mathcal{H}_N$ are nested inside the Cauchy horizon $\mathcal{H}_-$ and are tangent to $\mathcal{H}_-$ along the CNG $\mathcal{C}$. ($\mathcal{C}$ must be tangent to all the $\mathcal{H}_N$ because it is a CNG that returns smoothly onto itself, and this means that all events on it can be connected to themselves by a piece of $\mathcal{C}$ that traverses the wormhole any fixed number of times $N$ that one might desire. By contrast, for events on $\mathcal{H}_N$ that do not lie on $\mathcal{C}$, e.g., the event $\mathcal{P}$ on $\mathcal{H}_1$ in the figure, the CNG that joins them to themselves does not return on itself smoothly. Rather, it crosses itself at some finite angle. The CNG $\mathcal{C}_1$ through $\mathcal{P}$ is an example; others are discussed analytically in Secs. III, V A, and VI A.) As Fig. 1 shows, the Cauchy horizon $\mathcal{H}_-$ is the limit of $\mathcal{H}_N$ as $N \to \infty$. Accordingly, as was asserted above, every event on the Cauchy horizon is arbitrarily close to the identical end points of a CNG (end points that lie on $\mathcal{H}_N$ for $N$ arbitrarily large).

This relationship between the Cauchy horizon and the polarized hypersurfaces is not peculiar to the specific wormhole spacetime depicted in Fig. 1. It is generic. The $\mathcal{H}_N$ are always nested in such a way that the limit of $\mathcal{H}_N$ as $N \to \infty$ is $\mathcal{H}_-$. The proof is rather simple.

(i) Choose an arbitrary event $Q_-$ on $\mathcal{H}_-$, and then choose some other event $Q$ that is in the region with CTC's, and is arbitrarily close to $Q_-$. (ii) Through the event $Q$ there must pass a CTC. (iii) That CTC must make some number $n$ (not zero) of loops through the wormhole as it travels from $Q$ in a timelike fashion back to $Q$. (iv) By retracing that CTC over and over again we can turn it into a CTC $\mathcal{E}_N$ with an arbitrarily large number $N$ of loops through the wormhole. (v) We can then push $Q$ closer and closer to the event $Q_-$, deforming $\mathcal{E}_N$ continuously in the process but keeping its two ends attached to $Q$ and keeping it everywhere causal. Ultimately $\mathcal{E}_N$ will become a closed null geodesic, and we will not be able to push $Q$ any closer to $Q_-$ without forcing some piece of $\mathcal{E}_N$ to become spacelike. (vi) $Q$ now lies on $\mathcal{H}_N$, the polarized hypersurface of order $N$. Since $Q$ began arbitrarily close to $Q_-$ and is now even closer, this shows that arbitrarily close to any point $Q_-$ on $\mathcal{H}_-$ there is a piece of $\mathcal{H}_N$ with arbitrarily large $N$. In other words, $\mathcal{H}_-$ is the limit of $\mathcal{H}_N$ as $N \to \infty$.

This nesting of the $\mathcal{H}_N$ guarantees that, when any observer (e.g., one who moves along the world line $\mathcal{L}$ of Fig. 1) enters the region of CTC's, that observer will pass first through the Cauchy horizon $\mathcal{H}_-$, and then will pass sequentially through the various $\mathcal{H}_N$. At each of the $\mathcal{H}_N$ the observer will experience a strong peak of vacuum polarization, and between the $\mathcal{H}_N$ the vacuum polarization will be much weaker.

## B. Point-splitting regularization

In this paper we calculate the details of this vacuum polarization for a quantized, massless, conformally coupled scalar field $\phi$, using a point-splitting regularization[15] of the stress-energy tensor in the geometric-optics limit.

We do so not only at events immediately preceding the Cauchy horizon $\mathcal{H}_-$, but also at events that lie close to the polarized hypersurfaces $\mathcal{H}_N$, which are after the Cauchy horizon and in the region with CTC's.

What makes us confident that quantum field theory can be formulated in anything like its standard form in the region with CTC's? Our confidence comes from the following.

(i) It seems rather certain that, for a classical, massless scalar field $\phi$ in an asymptotically flat wormhole spacetime with CTC's, the Cauchy problem is well posed in this sense: For every choice of the standard initial data at past null infinity, there exists a unique solution of the scalar wave equation throughout the spacetime. The reasons for this are spelled out in Ref. 6, and a rigorous proof has been given by Friedman and Morris[7] for a specific example of such a spacetime (the example described in Fig. 4). (ii) This implies that we can define a complete set of modes of the classical field $\phi$ in the standard way at past null infinity, and can then propagate each of these modes throughout the spacetime, including the region with CTC's. These modes will satisfy standard orthogonality conditions with respect to the standard inner product, with the one unusual feature that the hypersurfaces on which the inner product is computed cannot everywhere be spacelike; see Fig. 5 of Ref. 6, and the associated discussion. (iii) The Fock space for the quantum field $\hat{\phi}$ can then be constructed in the standard manner in terms of these modes. (iv) The standard point-splitting procedure for evaluating the renormalized stress-energy tensor should then follow.

We have not yet explored this quantization procedure in full detail, so we are not absolutely certain that it goes through fully successfully. However, as yet we have seen no sign of any difficulties. If it fails in some as-yet-unseen way, then the analysis in this paper at least will still be correct before the Cauchy horizon and should correctly predict the strength of the divergence of the vacuum polarization as one approaches the horizon.

In our computation of the vacuum polarization, we shall not use a mode expansion of the field operator. Rather, we shall use, as the foundation of our calculation, a geometric-optics approximation to the Hadamard function. The Hadamard function is the following classical biscalar field, which depends on two points $x$ and $x'$ in spacetime and on the quantum state $| \Psi \rangle$ of the quantized scalar field $\phi$:

$$G^{(1)}(x, x') = \langle \Psi | \hat{\phi}(x)\hat{\phi}(x') + \hat{\phi}(x)\hat{\phi}(x') | \Psi \rangle . \quad (1)$$

Since the field operator $\hat{\phi}$ satisfies the conformally coupled scalar wave equation, so also does this Hadamard function, in both of its arguments:

$$[\Box_x + \tfrac{1}{6}R(x)]G^{(1)} = [\Box_{x'} + \tfrac{1}{6}R(x')]G^{(1)} = 0 . \quad (2)$$

The standard procedure for regularizing the Hadamard function[15] becomes especially simple when the event at which $T_{\mu\nu}$ is to be computed is surrounded by a neighborhood in which the spacetime curvature vanishes. This

is the case for all events in the spacetime of Fig. 1 and in most other model wormhole spacetimes currently being studied,[6,9,7,16] except for events precisely on the wormhole throat (which we shall avoid). It can also be made the case in generic wormhole spacetimes: Since we are interested only in the "divergent" behavior of the stress-energy tensor near polarized hypersurfaces, and not in its nondivergent parts, and since there is no reason to expect the divergent behavior to be affected by small, localized alterations in the spacetime curvature, in generic wormhole spacetimes we can "flatten" spacetime locally[17] in a tiny neighborhood around any event at which we wish to evaluate the stress-energy tensor.

In our chosen, curvature-free neighborhood, regularization of the Hadamard function reduces to simply subtracting off its flat-spacetime, vacuum-state value:[15]

$$G^{(1)}_{\text{reg}} = G^{(1)} - \frac{1}{4\pi^2\sigma_0} . \tag{3}$$

Here $\sigma_0$ is half the square of the infinitesimal vector separation between $x'$ and $x$.

The field's renormalized stress-energy tensor in the state $|\Psi\rangle$ is computed from this regularized Hadamard function using the relation[15]

$$T_{\mu\nu} = \lim_{x \to x'} \mathcal{D}_{\mu\nu} G^{(1)}_{\text{reg}} , \tag{4a}$$

where $\mathcal{D}_{\mu\nu}$ is the second-order differential operator

$$\mathcal{D}_{\mu\nu} = \frac{2}{3}\nabla_\mu\nabla_{\nu'} - \frac{1}{3}\nabla_\mu\nabla_\nu - \frac{1}{6}g_{\mu\nu}\nabla_\alpha\nabla^{\alpha'} . \tag{4b}$$

### C. Geometric-optics approximation to $G^{(1)}$

In this paper we deal with the unusual situation where $x$ and $x'$, though infinitesimally close to each other, nevertheless can be connected by an infinite number of geodesics $\mathcal{G}_N$, each characterized by an integer $N$ (positive, negative, or zero). Geodesic $\mathcal{G}_0$ reaches along the infinitesimal vectorial separation from $x'$ to $x$. For positive $N$, geodesic $\mathcal{G}_N$ begins at $x'$ and, traveling always locally forward in time, traverses the wormhole from mouth 2 to mouth 1 $N$ times before arriving at $x$. The dashed curve $\mathcal{G}_1$ in Fig. 2 is an example, for $N = 1$. For negative $N$, $\mathcal{G}_N$ begins at $x'$ and, traveling always locally backward in time, traverses the wormhole from mouth 1 to mouth 2 $N$ times before arriving at $x$. The dashed curve $\mathcal{G}_{-1}$ in Fig. 2 is an example.

For the points $x$, $x'$ that we shall consider (e.g., those of Fig. 2), two or more of the wormhole-traversing geodesics $\mathcal{G}_N$ will be very nearly null (e.g., $\mathcal{G}_1$ and $\mathcal{G}_{-1}$ in Fig. 2). In this situation, the Hadamard function $G^{(1)}$ [which can be thought of as evolving via the wave equations (2)] contains huge contributions produced by propagation along routes very close to each of the nearly null $\mathcal{G}_N$. These contributions can be described by a geometric-optics expression, which is an obvious generalization of the standard Hadamard expansion[18] of $G^{(1)}$ (see Sec. III):
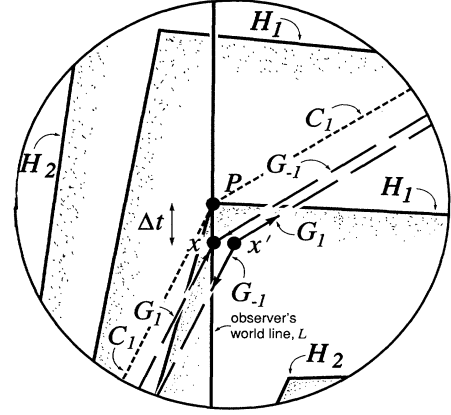


FIG. 2.   Blowup of the spacetime region of Fig. 1, near the event $\mathcal{P}$.

$$G^{(1)}_{\text{reg}} = \sum_{N \neq 0} \frac{\Delta_N^{1/2}}{4\pi^2} \left( \frac{1}{\sigma_N} + v_N \ln|\sigma_N| + w_N \right) . \tag{5}$$

Here the sum is over all nearly null geodesics $\mathcal{G}_N$ that go from $x'$ to $x$ [except $\mathcal{G}_0$, whose contributions are removed by the regularization of Eq. (3)]; $\sigma_N$, the $N$th geodetic interval between $x$ and $x'$, is equal to 1/2 the square of the proper distance along $\mathcal{G}_N$ from $x'$ to $x$, multiplied by $-1$ if $\mathcal{G}_N$ is timelike and $+1$ if it is spacelike; and $\Delta_N$, $v_N$, and $w_N$ are functions which, unlike $1/\sigma_N$, vary smoothly as $x$ moves through the light cone of $x'$ (i.e., as $\mathcal{G}_N$ switches from spacelike to null to timelike).

For points $x$ very close to the $N$th polarized hypersurface $\mathcal{H}_N$, and for $x'$ arbitrarily close to $x$ (e.g., Fig. 2 with $N = 1$), the geodesics $\mathcal{G}_{\pm N}$ are very nearly null, the geodetic intervals $\sigma_{\pm N}$ are infinitesimally small, $1/\sigma_{\pm N}$ are arbitrarily large, and correspondingly the order-$\pm N$ contributions to $G^{(1)}$ and to $T_{\mu\nu}$ are arbitrarily large (divergent). Since the divergence is produced by the leading $1/\sigma_{\pm N}$ part of $G^{(1)}$ and is unaffected by the part $w_{\pm N}$ that depends on the state $|\Psi\rangle$ of the field,[18] the divergence is an intrinsic feature of the field's vacuum. It is a vacuum-polarization divergence.

### D. Order-of-magnitude evaluation of $G^{(1)}$ and $T^{\mu\nu}$

We shall now evaluate the strength of the vacuum polarization divergence in order of magnitude.

Consider an event $x$ arbitrarily close to the polarized hypersurface $\mathcal{H}_N$ in any wormhole spacetime with closed timelike curves, and choose an observer whose world line passes through $x$ and then, a tiny proper time $\Delta t$ later, passes through $\mathcal{H}_N$ (cf. Fig. 2). (We use $t$ to denote the observer's proper time, and $T$ to denote Lorentz coordinate time in the flat region of the spacetime of Figs. 1 and 2. For the special case of that spacetime, and for the observer's world line $\mathcal{L}$ shown in Fig. 1, these two times

are equal: $t = T$.) Denote by $D$ the spatial length of $\mathcal{G}_N$ as measured in the observer's reference frame, as it makes a trip from the vicinity of $x$ and $x'$, through the wormhole once, and back to the vicinity of $x$ and $x'$. (In the spacetime of Figs. 1 and 2, and for any split points $x'$, $x$ near that portion of $\mathcal{H}_N$ which is shown in Fig. 1, $D$ is roughly the same as the length of the CNG $\mathcal{C}$ from which the Cauchy horizon's null generators spring; i.e., it is roughly equal to the separation between the two wormholes at the moment when the Cauchy horizon comes into being.)

It is easy to convince oneself, by an argument whose spirit is embodied in "$\sigma \sim T^2 - X^2 = (T+X)(T-X) \sim D\Delta t$," that for $x'$ much closer to $x$ than $x$ is to $\mathcal{H}_N$, the geodetic intervals between $x'$ and $x$ are

$$\sigma_{\pm N} \sim D\Delta t . \tag{6a}$$

Note that as $\Delta t$ goes to zero, i.e., as $x$ approaches the polarized hypersurface $\mathcal{H}_N$, $\sigma_{\pm N}$ go to zero and thus the regularized Hadamard function (5) diverges to infinity. The strength of $G^{(1)}$'s divergence is proportional to the values of the function $\Delta_{\pm N}$ in the vicinity of $x$. This function, called the "scalarized Van Vleck–Morette determinant," is (cf. Sec. III) a measure of the defocusing effects that the wormhole exerts on the amplitude of a classical, high-frequency scalar wave which propagates along a null geodesic that closely parallels $\mathcal{G}_{\pm N}$, beginning near $x'$, $x$, passing through the wormhole $N$ times, and ending back near $x'$, $x$. More specifically, $\Delta_{\pm N}^{1/2}$ is the amplitude that the wave has after its trip, divided by the amplitude the wave would have if there were no defocusing by the wormhole. Since the wormhole acts like a diverging lens with focal length of order $b \equiv$(radius of wormhole throat),[2] each wormhole traversal followed by propagation a substantial fraction of the way toward the next traversal produces a defocusing-induced amplitude decrease of order $b/D$. (Here and throughout we presume that $b/D \ll 1$.) If $x$ is far from both wormhole mouths, there will be $N$ such defocusing factors, so

$$\Delta_{\pm N}^{1/2} \sim \left(\frac{b}{D}\right)^N \text{ if } x \text{ is far from both mouths.} \tag{6b}$$

If $x$ is very close to either mouth, then one of the geodesics $\mathcal{G}_{\pm N}$ will travel a negligible distance after its last ($N$th) wormhole traversal, and thus will have $\Delta^{1/2} \sim (b/D)^{(N-1)}$, while the other will travel such a tiny distance before the first wormhole traversal that the first traversal will produce negligible defocusing, and again $\Delta^{1/2} \sim (b/D)^{N-1}$. Thus

$$\Delta_{\pm N}^{1/2} \sim \left(\frac{b}{D}\right)^{(N-1)} \text{ if } x \text{ is near either mouth.} \tag{6c}$$

The order-of-magnitude values (6a)—(6c) of $\sigma_{\pm N}$ and $\Delta_{\pm N}$ imply the following magnitude for the Hadamard function near the polarized hypersurface $\mathcal{H}_N$:

$$G_{\text{reg}}^{(1)} \sim \frac{\Delta_{\pm N}^{1/2}}{\sigma_{\pm N}} \sim \left(\frac{b}{D}\right)^{N \text{ or } (N-1)} \frac{1}{D\Delta t} . \tag{7}$$

When $G_{\text{reg}}^{(1)}$ is differentiated twice to produce the stress-energy tensor [Eqs. (4)], the result is a factor $(\Delta t)^3$ in the denominator rather than $\Delta t$:

$$T^{\mu\nu} \sim \left(\frac{b}{D}\right)^{N \text{ or } (N-1)} \frac{1}{D(\Delta t)^3} . \tag{8}$$

Here the power is $N$ if the point $x$ is far from either mouth of the wormhole, and $N - 1$ if it is close to a mouth.

### E. Physical effects of the "divergent" $T^{\mu\nu}$; conjecture that quantum gravity cuts off the divergence and permits CTC's

To make physical sense out of these order-of-magnitude estimates, it is helpful to convert from the natural units, $c = G = \hbar = 1$, in which the above formulas are written, to cgs units (but with $c$ still unity). This can be done by noting that the vacuum polarization is proportional to Planck's constant $\hbar$, or equivalently to the product of the Planck length $l_P = \sqrt{G\hbar/c^3}$ and the Planck mass $m_P = \sqrt{\hbar c/G}$. Correspondingly, expression (8) becomes

$$T^{\mu\nu} \sim \left(\frac{b}{D}\right)^{N \text{ or } (N-1)} \left(\frac{l_P}{D}\right) \left(\frac{m_P}{(\Delta t)^3}\right) . \tag{9a}$$

This scalar-field stress energy acts back on the spacetime to produce (via the Einstein field equation) a spacetime curvature with magnitude

$$R_{\mu\rho\nu\sigma} \sim GT_{\mu\nu} \sim \left(\frac{b}{D}\right)^{N \text{ or } (N-1)} \left(\frac{l_P}{D}\right) \left(\frac{l_P}{(\Delta t)^3}\right) . \tag{9b}$$

The corresponding metric perturbation (equal to the fractional change of length $\delta L/L$ that an idealized, broadband gravitational-wave detector would undergo, as it is carried by our chosen observer up to time $\Delta t$) is

$$\frac{\delta L}{L} \simeq \delta g_{\mu\nu}^{\text{VP}} \sim \left(\frac{b}{D}\right)^{N \text{ or } (N-1)} \left(\frac{l_P}{D}\right) \left(\frac{l_P}{\Delta t}\right) . \tag{9c}$$

This is the divergence as the observer approaches the $N$th polarized hypersurface $\mathcal{H}_N$. The divergence will be far weaker than this as the observer approaches the Cauchy horizon $\mathcal{H}_-$ (cf. Fig. 1), except at the CNG $\mathcal{C}$ from which the horizon generators spring: because all the $\mathcal{H}_N$ are tangent to $\mathcal{H}_-$ at $\mathcal{C}$, the dominant divergence at $\mathcal{C}$ will have the form (9) with $N = 1$.

The authors' argument, suggesting that this divergence may be cut off by quantum gravity long before it becomes of order unity (and thus, at the Cauchy horizon, long before it can prevent the creation of CTC's), proceeds as follows.

On any time scale $\Delta t$ and in any classical spacetime, flat or curved, quantum gravity presumably produces fluctuations of the curvature and metric with

magnitude[19]

$$\delta R^{QG}_{\mu\nu\rho\sigma} \gtrsim \frac{l_P}{(\Delta t)^3}, \quad \delta g^{QG}_{\mu\nu} \gtrsim \frac{l_P}{\Delta t} . \quad (10)$$

Note that at all times $\Delta t$ these quantum gravity fluctuations are larger than the vacuum-polarization-induced fluctuations (9) by a factor

$$\frac{\delta g^{QG}_{\mu\nu}}{\delta g^{VP}_{\mu\nu}} \gtrsim \frac{D}{l_P} \left( \frac{D}{b} \right)^{N \text{ or } (N-1)} . \quad (11)$$

Since we have presumed the wormhole throat to be tiny compared to the distance between the wormhole mouths, $b \ll D$, and since the horizon or polarized hypersurface must always have $N \geq 1$ in Eqs. (9), the quantum-gravity fluctuations dominate over the scalar field's vacuum-polarization effects by a factor $\gtrsim D/l_P$.

This quantum-gravity dominance does not necessarily mean that the vacuum polarization is insignificant. After all, the quantum-gravity fluctuations (10) have vacuum expectation values that are tiny compared to the fluctuations themselves—in fact, that are probably of the same order as the vacuum polarization effects (9) which we have computed, so long as $\Delta t \gtrsim l_P$. Thus, we must be concerned about the strength of the vacuum polarization.

The vacuum polarization's energy density

$$T^{00} \sim - \left( \frac{b}{D} \right)^{N \text{ or } (N-1)} \left( \frac{l_P}{D} \right) \left( \frac{m_P}{(\Delta t)^3} \right) \quad (12)$$

is plotted as a function of the observer's proper time $t$ in Fig. 3(a). (The minus sign comes from a more careful examination of the derivatives of $1/\Delta t$ than we gave above; cf. Secs. V D and VI D.) The cross-hatched region in Fig. 3(a) is that, $|\Delta t| \lesssim l_P$, in which classical spacetime does not exist and therefore Eq. (12) fails. Presumably quantum gravity causes some sort of probabilistic interpolation of the predictions of Eq. (12) through this region, from the extremely negative energy density just before the horizon or polarized hypersurface to the extremely positive energy density just afterward.

The form of the energy density near the horizon or polarized hypersurface is that of a dipole layer of energy: a highly localized, negative energy density on one side, and a highly localized, equal-in-magnitude, but positive energy density on the other.

If, as we have argued, quantum gravity produces a probabilistic interpolation of the energy density at $|\Delta t| \lesssim l_P$, what will be the nature and magnitude of the tidal gravitational forces felt by our observer as he/she passes through the horizon or polarized hypersurface? If the observer carries an idealized gravitational-wave detector with perfect, broadband frequency response, the detector will exhibit the tidal-gravity-induced strain shown in Fig. 3(b). This strain is the second time integral of the Riemann tensor (9b), with interpolation through the quantum-gravity region. The maximum strain is given, in order of magnitude, by Eq. (9c) (which is valid only before the horizon or polarized hypersurface is reached), with $\Delta t \sim l_P$:

$$\left( \frac{\delta L}{L} \right)_{\max} \sim (\delta g^{VP}_{\mu\nu})_{\max} \sim \left( \frac{b}{D} \right)^{N \text{ or } (N-1)} \left( \frac{l_P}{D} \right) . \quad (13)$$

Since $N \geq 1$, for a macroscopic wormhole with, say, $D \gtrsim 1$ m, this maximum strain is $(\Delta L/L)_{\max} \lesssim 10^{-35}$. This is far too small to be detected with even the most advanced modern technology. Thus, our observer will not notice at all the tidal effects of the "divergent" vacuum polarization as he/she passes through the polarized hypersurface.

Although the tidal effects of the vacuum polarization are negligible, the numerical value of the maximum energy density is rather impressive: This maximum is largest near the wormhole throat, and near the horizon's CNG $\mathcal{C}$ or near the first polarized hypersurface, $N = 1$. There the power in Eq. (13) is $N - 1 = 0$, so for a wormhole separation of one meter, the maximum energy density

$$T^{00}_{\max} \sim \left( \frac{l_P}{D} \right) \left( \frac{m_P}{(\Delta t)^3} \right)_{\Delta t = l_P} = \left( \frac{l_P}{D} \right) \left( \frac{m_P}{l_P^3} \right) \quad (14)$$

is $l_P/D \sim 10^{-35}$ of the Planck density $m_P/l_P^3$; i.e., it is $T^{00}_{\max} \sim 10^{49}$ g/cm$^3$. In the spacetime of Fig. 1, this energy density is accompanied by an energy flux of the same magnitude; see Secs. V D, V E, VI D, and VI E for details. By integrating the energy flux $T^{0r} \sim (l_P/D)[m_P/(\Delta t)^3]$
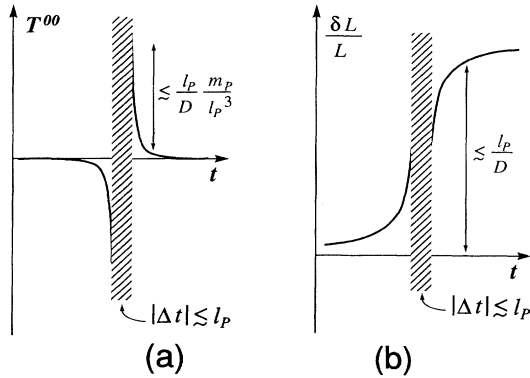
FIG. 3. (a) The vacuum-polarization energy density measured by an observer who moves along the world line $\mathcal{L}$ of Figs. 1 and 2, as the observer nears and passes through the $N$th polarized hypersurface $\mathcal{H}_N$. Shown stippled is the region so close to $\mathcal{H}_N$ ( $|\delta t| \lesssim l_P$) that the classical concept of time makes no sense. Presumably quantum gravity halts and smears out the divergence of the energy density in this region. (b) The strain $\delta L/L$ produced in an idealized gravitational-wave detector by the vacuum polarization's spacetime curvature, as the detector moves along the world line $\mathcal{L}$.

in time from $\Delta t = -\infty$ to $\Delta t = -l_P$, and integrating in space over a sphere enclosing the wormhole throat, we obtain for the total vacuum-polarization energy that flows through the wormhole just before the polarized hypersurface $\mathcal{H}_1$

$$\Delta M_1 \sim \left(\frac{1}{G}\right)\left(\frac{b^2}{D}\right) . \tag{15a}$$

Notice that this total energy transfer is independent of Planck's constant, and is of order $b/D$ times the mass of a *black* hole whose horizon radius is equal to the radius of our *wormhole*.

For $b \ll D$, the mass transfer is so small that it is unlikely to exert any significant effect on the wormhole; and whatever effect it has will likely be undone by the equal and opposite-signed mass transfer that occurs immediately after the polarized hypersurface $\mathcal{H}_1$. For $b \sim D$, the energy transfer is of order $b/G$, which is roughly large enough to create a black-hole-type horizon around one of the mouths and very possibly large enough to seal off the wormhole. However, the reversal of the mass transfer begins so quickly after the dangerous value $b/G$ is reached, and the net transfer is of order $b/G$ for such a brief time (a few Planck times), that it is far from obvious that a black-hole-type horizon will be able to form before the pulse of mass transfer is over.

For the other polarized hypersurfaces $\mathcal{H}_N$ the mass transfer is even smaller than for $\mathcal{H}_1$: smaller by a factor $(b/D)^{N-1}$; and if one integrates the mass transfer only up to the Cauchy horizon $\mathcal{H}_-$, and not up to $\mathcal{H}_N$ with finite $N$, the mass transfer is smaller than the Planck mass:

$$\Delta M_- \sim (b/D)m_P \tag{15b}$$

(Secs. V E and VI E).

Although the detailed computations of the remainder of this paper are restricted to the specific wormhole
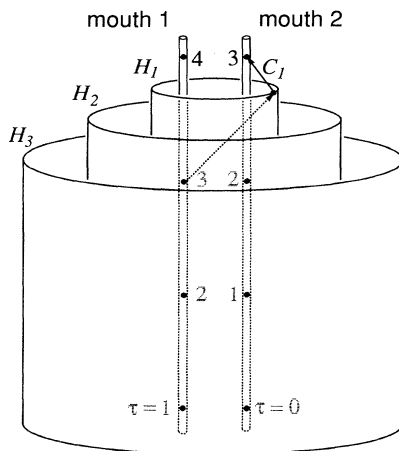


FIG. 4. The spacetime of an "eternal time machine." This spacetime is analyzed in some detail in Refs. 6, 7, and 16.

spacetime of Fig. 1, the above discussion is valid for any wormhole spacetime with closed timelike curves. For example, it can be applied to the "eternal time-machine" spacetime of Fig. 4, in which there are closed timelike curves everywhere and no Cauchy horizon. As Frolov and Novikov[16] show, in this spacetime the $\mathcal{H}_N$ are a series of static, nested, ellipsoidally shaped, timelike hypersurfaces. An observer who passes at high speed, e.g., $v \simeq 0.5$, through any of these $\mathcal{H}_N$ should see a vacuum-polarization energy density with magnitude given by expression (12), and with accompanying spacetime curvature and metric perturbations given by expressions (9b) and (9c).

### F. Hawking's chronology protection conjecture

Hawking[13] objects to the above discussion on grounds that the location at which semiclassical theory (quantum field theory in curved spacetime) breaks down should be observer independent, whereas the above discussion asserts a breakdown at $\Delta t \sim l_P$, and the time $\Delta t$ to the Cauchy horizon (or a polarized hypersurface) depends on the chosen observer, i.e., the chosen reference frame. We agree, of course.

The arguments (e.g., those in Ref 19) suggesting that classical spacetime breaks down at $\Delta t \sim l_P$, when examined closely, presume that $\Delta t$ is the proper time between two neighboring, spacelike hypersurfaces, and that the spacetime geometry is being averaged not only over the time $\Delta t$ but also over a spatial region of 3-volume $(\Delta t)^3$. These arguments entail a preferred reference frame: the frame in which the chosen hypersurfaces are slices of simultaneity. However, the issue that concerns us in this paper is not how well defined is the time between two chosen spacelike hypersurfaces, but rather how well defined is the spacetime geometry in the vicinities of null geodesics (those along which the Hadamard function $G^{(1)}$ and associated vacuum fluctuations propagate). In discussing this issue, we are to squeeze smaller and smaller the thickness $\Delta t$ of the region preceding and following the null geodesic (as seen in some reference frame), while allowing the spacetime region to remain macroscopic along the geodesic. The issue is how small can $\Delta t$ be squeezed until fluctuations of geometry make the geodesic and its neighbors become so ill defined as to invalidate our computation of the vacuum polarization—i.e., so ill defined as to cause a breakdown of the semiclassical theory (quantum field theory in curved spacetime) on which our computation is based.

Since this $\Delta t$ is frame dependent (an inevitable consequence of the nullness of the geodesic), any assertion that the breakdown occurs at $\Delta t \sim l_P$ can be true only in some preferred reference frame. Since the location of the breakdown is defined only in rough order of magnitude, the preferred frame will be defined only in rough order of magnitude. The authors' conjecture (preceding section) tacitly assumes that the preferred frame is that associated with the macroscopic features of spacetime which

are driving the formation of the CTC's. For the wormhole spacetime of Fig. 1, that preferred frame is the rest frame of either wormhole mouth.

Our guess of the preferred frame could be wrong, and Hawking argues that it is. He thinks it likely that the semiclassical theory breaks down at points $x$ where the shortest invariant geodetic interval $\sigma(x, x)$ connecting $x$ to itself is $l_P^2$. Since $\sigma(x, x) \sim D\Delta t$, this corresponds to a breakdown at $D\Delta t \sim l_P^2$ (and thus, if $D \sim 1$ m, at $\Delta t \sim 10^{-35} l_P$). If Hawking is correct, then before semiclassical theory fails, $\delta g_{\mu\nu}^{\rm VP}$ becomes of order unity near the closed null geodesic $\mathcal{C}$ from which the Cauchy horizon springs, and being so large, this $\delta g_{\mu\nu}^{\rm VP}$ might (as Hawking speculates) change the classical spacetime structure enough to protect it against CTC's.

There is a preferred reference frame in which the arguments of the preceding section give Hawking's location $D\Delta t \sim l_P^2$ for the breakdown of semiclassical theory. This is a frame in which the observer is moving so rapidly along and near the CNG $\mathcal{C}$ that he/she sees the spatial length $D$ of $\mathcal{C}$ Lorentz contracted to the Planck length. In this frame, and only in this frame, Hawking's location for breakdown corresponds to $\Delta t \sim l_P$.

At first sight, this choice of preferred frame looks rather appealing: After all, why should quantum gravity care at all about the rest frame of the macroscopically huge wormhole mouths (or whatever else may be driving the formation of CTC's)? Should not quantum gravity be atuned only to physics occurring on submicroscopic scales $\sim l_P$, and thus should not it pick out its preferred frame by a submicroscopic criterion such as the frame in which $D \sim l_P$?

At second sight, the Hawking choice of preferred frame has a peculiar (though not entirely outrageous) implication: The Hawking choice suggests that in the vicinity of the CNG $\mathcal{C}$, local fluctuations of geometry (as seen, e.g., in the rest frame of a wormhole mouth) have negligible net influence on the null geodesics along which the Hadamard function $G^{(1)}$ and its associated diverging field fluctuations propagate. Only global fluctuations of geometry, which are coherent over the scale of the CNG $\mathcal{C}$ (and which are Lorentz contracted into a Planck length along $\mathcal{C}$ as seen in the Hawking frame) would appear to impede the existence of a well-defined, classical, spacetime structure along $\mathcal{C}$. This by itself is intriguing. However, it suggests, by extension, that in the vicinity of a null surface that has no closed null geodesics (i.e., in the vicinity of any ordinary light cone), local fluctuations of geometry also should not affect the well definedness of the classical (null) spacetime structure. In this case, there are no global fluctuations of geometry, so it would seem that quantum gravity leaves the classical spacetime structure well defined arbitrarily close to the light cone—when one is paying attention in some sense to the entire light cone and not just to a segment of it. This seems rather strange; but, of course, the arguments that have led to it are awfully fuzzy.

The difference between the Hawking conjecture and ours is so huge (a factor $10^{35}$ in where semiclassical theory breaks down when $D \sim 1$ m), that there might be some hope of seeing which (if either) is correct according to various candidate quantum theories of gravity. Indeed, the attempt to distinguish between the two conjectures might provide useful insight into the candidate theories themselves.

## III. HADAMARD FUNCTION IN THE GEOMETRIC-OPTICS LIMIT

In this section we sketch a derivation of the geometric-optics expansion (5) of the regularized Hadamard function in an arbitrary wormhole spacetime with closed timelike curves.

We begin with the unregularized Hadamard function

$$G^{(1)}(x, x') = \langle \Psi \mid \hat{\phi}(x)\hat{\phi}(x') + \hat{\phi}(x)\hat{\phi}(x') \mid \Psi \rangle , \qquad (16)$$

and throughout our analysis we constrain the point $x'$ to not lie on the Cauchy horizon or on any polarized hypersurface or (for pedagogical simplicity) at a location where there is spacetime curvature. (At the end of our computation of $T^{\mu\nu}$, we will let the coalesced points $x$ and $x'$ approach $\mathcal{H}_-$ or one of the $\mathcal{H}_N$.) Then, on some arbitrary, local spacelike hypersurface $\mathcal{S}$ surrounding $x'$ there will be a neighborhood $\mathcal{N}(x')$ that is devoid of curvature and is not pierced by $\mathcal{H}_-$ or any $\mathcal{H}_N$. We initially choose the point $x$ to lie in this $\mathcal{N}(x')$ and extremely close to $x$. For this choice, the singular part of the Hadamard function must have the standard flat-spacetime form

$$G^{(1)} = \frac{1}{4\pi^2 \sigma} , \qquad (17)$$

in the limit as $x$ approaches $x'$. Here $\sigma$ is the geodetic interval between $x'$ and $x$ (half the square of the proper distance along the spacelike geodesic from $x'$ to $x$).

To see that this singularity structure is correct, despite the presence of CTC's, imagine expanding the field operator in a complete set of modes such that those ultra-high-frequency modes which contribute to $G^{(1)}$, for the chosen $x'$ and $x$, are wave packets that do not extend, on the spacelike hypersurface $\mathcal{S}$, outside the neighborhood $\mathcal{N}(x')$. [The modes may, however, have other nonvanishing components at other locations on $\mathcal{S}$; such components may be produced by propagation of the component from $\mathcal{N}(x')$ through the wormhole and back to $\mathcal{S}$. These other components will have no influence on the form of $G^{(1)}$ for $x$ in $\mathcal{N}(x')$ if they are separated from $\mathcal{N}(x')$ by regions of $\mathcal{S}$ in which the modes vanish. That the modes can be selected in this way is implied by the fact that $\mathcal{N}(x')$ is bounded away from all the $\mathcal{H}_N$; cf. the discussion below of the evolution of $G^{(1)}$.] The components of these modes in $\mathcal{N}(x')$ cannot feel any effects of spacetime curvature, nor any effects of CTC's. They, therefore, must produce the same singularity structure for the Hadamard function, Eq. (17), as they would do in flat, CTC-free spacetime.

We now ask the following question: What singularity structure is enforced on $G^{(1)}(x, x')$, for fixed $x'$ and for $x$ now allowed to range over the entire spacetime, by the singular behavior (17) for $x$ in $\mathcal{N}(x')$? We answer this question by evolving $G^{(1)}(x', x)$ as a function of $x$ via the wave equation (2). In this evolution we do not care about smoothly varying pieces of $G^{(1)}$; we are only concerned with the singular pieces. The singular pieces are composed of arbitrarily high frequencies, and thus evolve in a geometric-optics manner. Since the singularity initially [in the neighborhood $\mathcal{N}(x')$] is confined to the point $x = x'$, the geometric-optics-evolved singularity will be confined to $x$ on the future and past light cones of $x'$. Because our initial $x'$ was bounded away from any polarized hypersurfaces, its future and past light cones cannot travel through the wormhole multiple times and then return to $x'$; the singularity structure thus cannot propagate back to corrupt the initial data.

The solution to the scalar wave equation (2) in the vicinity of the future and past light cones of $x'$ is well known. It has the Hadamard normal form[18]

$$G^{(1)} = \frac{\Delta^{1/2}}{4\pi^2} \left( \frac{1}{\sigma} + v \ln |\sigma| + w \right) . \tag{18}$$

Here $\sigma$ is the geodetic interval between $x'$ and $x$; $\Delta$ is the scalarized Van Vleck–Morette determinant

$$\Delta \equiv \frac{\det \| \sigma_{;\mu\nu'} \|}{\sqrt{g(x)g(x')}} \tag{19}$$

with $g(x)$ and $g(x')$ the determinants of the covariant components of the metric tensor at $x$ and $x'$; and $v$ and $w$ are functions that, like $\Delta$, are smooth across the light cone. The $v \ln |\sigma|$ term is a "tail" produced on the singularity structure by scattering of the $1/\sigma$ piece off the spacetime curvature, and thus is absent in our initial data in the absolutely flat region $\mathcal{N}(x')$. The singular pieces $\Delta^{1/2}(1/\sigma + v \ln |\sigma|)$ are determined fully by the chosen points $x$, $x'$ and the geometric and topological structure of spacetime,[18] and thus are associated entirely with vacuum fluctuations of the field $\phi$. By contrast, the completely smooth piece $\Delta^{1/2}w$ (which does not interest us) depends not only on $x$, $x'$, and the geometric and topological structure of spacetime, but also on the state $|\Psi\rangle$ of the field.

Return, now, to points $x$ that lie in the neighborhood $\mathcal{N}(x')$. The Hadamard function at these points will be dominated by the initial singular contribution (17), but it will also be influenced by weaker singular contributions associated with pieces of the past and future light cone of $x'$ that have propagated through the wormhole and returned to the vicinity of (but outside of) $\mathcal{N}(x')$. For the spacetime of Fig. 1, each such piece of the light cone on $\mathcal{S}$, near $\mathcal{N}(x')$, can be characterized by the number of times it has traversed the wormhole (with negative numbers for pieces of the past light cone, and positive numbers for pieces of the future light cone). Correspondingly, we can write $G^{(1)}$ for $x$ in $\mathcal{N}(x')$ in the form

$$G^{(1)} = \sum_{N=-\infty}^{+\infty} \frac{\Delta_N^{1/2}}{4\pi^2} \left( \frac{1}{\sigma_N} + v_N \ln |\sigma_N| + w_N \right) , \tag{20}$$

where the subscript $N$ denotes the contribution from the singularity structure associated with piece $N$ of the light cone near $\mathcal{N}(x')$.

This Hadamard function is regularized by subtracting off the initial, $N = 0$, singular piece [Eq. (17)]. By noting that $v_0$ vanishes and absorbing the uninteresting $w_0$ into the other $w_N$'s, we bring the regularized Hadamard function inside $\mathcal{N}(x')$ into the form (5) used in Sec. II C:

$$G_{\text{reg}}^{(1)} = \sum_{N \neq 0} \frac{\Delta_N^{1/2}}{4\pi^2} \left( \frac{1}{\sigma_N} + v_N \ln |\sigma_N| + w_N \right) . \tag{21}$$

This Hadamard function is regularized in the sense that, when the points $x$ and $x'$ are pushed together but are kept away from the polarized hypersurfaces $\mathcal{H}_N$, it remains finite.

As we have seen in Sec. II, it is the $\Delta_N^{1/2}/\sigma_N$ pieces of this regularized Hadamard function that produce the dominant divergent behavior of $T^{\mu\nu}$ near the Cauchy horizon and the polarized hypersurfaces. Correspondingly, in the following sections of this paper we shall need to compute the $N$th geodetic interval $\sigma_N$ between points $x'$ and $x$ that are very nearly on top of each other, and also the $N$th scalarized Van Vleck–Morette determinant $\Delta_N$.

To compute $\sigma_N$ we shall proceed as follows: (i) construct the unique geodesic $\mathcal{G}_N$ that begins at $x'$, goes forward in local time if $N$ is positive and backward if $N$ is negative, passes through the wormhole $|N|$ times, and then ends at $x$; and then (ii) use the definition of the geodetic interval to evaluate $\sigma_N$: half the square of the length of the geodesic $\mathcal{G}_N$ times $-1$ if $\mathcal{G}_N$ is timelike and $+1$ if it is spacelike.

It would be unpleasant if we had to compute $\Delta_N$ from its definition, Eq. (19), with $\sigma$ replaced by $\sigma_N$: we would have to evaluate $\sigma_N$ for a bundle of geodesics surrounding $\mathcal{G}_N$ and then differentiate twice. Fortunately, $\Delta_N$ can be computed, instead, by integrating an ordinary differential equation along the geodesic $\mathcal{G}_N$. This ordinary differential equation is a straightforward rewrite of Eq. (1.63) of Ref. 18. If $\zeta$ is an arbitrary affine parameter along $\mathcal{G}_N$, $d/d\zeta$ is the corresponding tangent vector to $\mathcal{G}_N$, and $\theta \equiv \nabla \cdot d/d\zeta$ is the corresponding expansion of a bundle of geodesics around $\mathcal{G}_N$ that all emanate from $x'$ (computable using the standard equations of geometric optics), then $\Delta_N$ is the solution to the differential equation

$$\frac{d\Delta}{d \ln \zeta} = (3 - \theta\zeta)\Delta . \tag{22}$$

The initial value of $\Delta$ for the integration is $\Delta = 1$ in the flat-spacetime region surrounding $x'$ (where $\theta = 3$), and $\Delta_N$ is the value that the integration yields at $x$, the end point of $\mathcal{G}_N$.

For the specific spacetime of this paper (Fig. 1), even this integration is more complicated than necessary. We shall evaluate $\Delta_N$ instead by using the fact that it appears not only in the regularized Hadamard function, but also in the symmetric (half-advanced plus half-retarded) propagator for a classical scalar wave:[18]

$$\bar{G}(x, x') = \sum_{N=-\infty}^{+\infty} \frac{\Delta_N^{1/2}}{8\pi}[\delta(\sigma_N) - v_N H(-\sigma_N)] \ . \qquad (23)$$

Here $\delta$ is the Dirac delta function and $H$ is its integral, the Heaviside function [$H(y) = -1$ for $y < 0$, $+1$ for $y > 0$]. When (as in our case) the geodesic $\mathcal{G}_N$ from $x'$ to $x$ is very nearly null (for example, in Figs. 1 and 2, $\mathcal{G}_1$ is very nearly the same as the closed null geodesic $\mathcal{C}_1$), then the value of $\Delta_N$ in the regularized Hadamard function (21) will be very nearly the same as the value that appears along the light cone in the propagator (23); and that value in turn is the ratio of the light-cone part of the propagator in the chosen spacetime to the propagator in flat spacetime.

This justifies the following method of computing $\Delta_N$. (i) Begin with an ultra-high-frequency, classical scalar wave $\psi$ emitted from the vicinity of $x'$. Take the wave's amplitude, in the initial, flat-spacetime region near $x'$, to be $\psi = 1/\zeta$, where $\zeta$ is affine parameter. (ii) Propagate the wave, using elementary geometric-optics considerations [which are equivalent to the light-cone part of the propagator (23)], along a null geodesic that is very close to $\mathcal{G}_N$. Propagate the wave through the wormhole $N$ times, and back to the vicinity of $x'$ and $x$—a total affine parameter distance $\zeta_N$. (iii) Then $\Delta_N^{1/2}$ will be given by the ratio of the resulting wave amplitude $\psi_N$ at its final point to the amplitude $1/\zeta_N$ that the wave would have had if it propagated through flat spacetime:

$$\Delta_N^{1/2} = \zeta_N \psi_N \ . \qquad (24)$$

We shall use this method in Secs. V B and VI B to evaluate $\Delta_N$ in the spacetime of Figs. 1 and 2.

## IV. SPACETIME GEOMETRY

In this section we shall spell out, in greater detail than heretofore, the geometry of the wormhole spacetime (Figs. 1 and 2) in which we carry out our detailed calculations.

The spacetime is constructed in the following manner [cf. Sec. II and Fig. 3(b) of Ref. 6]: In flat, Minkowskii spacetime with Lorentz coordinates $(T, X, Y, Z)$, identify two world lines parametrized by their proper times $\tau$, which will become the right edge of mouth 1 and the left edge of mouth 2 (cf. Fig. 1). The first world line is at rest at the origin of the Lorentz coordinate system,

$$T = \tau, \quad X = Y = Z = 0 \ , \qquad (25a)$$

and the second world line moves with speed $\beta$ toward the first:

$$T = D + \gamma\tau, \quad X = D - \beta\gamma\tau, \quad Y = Z = 0 \ . \qquad (25b)$$

Here, as usual, $\gamma = 1/\sqrt{1 - \beta^2}$. The origins $\tau = 0$ of $\tau$ on the two world lines are so chosen that (i) they are separated by the null line $X = T$ (which will later become the curve $\mathcal{C}$ from which the Cauchy horizon springs, cf. Fig. 1), and (ii) they have a spatial separation $D$. Introduce a second Lorentz coordinate system, one in which the second world line is at rest at the origin:

$$X' = \gamma(X - D) + \beta\gamma(T - D), \quad Y' = Y, \quad Z' = Z \ , \qquad (26)$$

$$T' = \gamma(T - D) + \beta\gamma(X - D) \ .$$

Cut out of the Minkowskii spacetime the world tube of a ball with radius $b$ and with right edge attached to the first world line,

$$(X + b)^2 + Y^2 + Z^2 = b^2 \ , \qquad (27a)$$

and similarly cut out the world tube of a second ball with left edge attached to the second world line,

$$(X' - b)^2 + Y'^2 + Z'^2 = b^2 \ . \qquad (27b)$$

These two balls become mouth 1 and mouth 2 of the infinitesimally thin wormhole, when one identifies the following events on them:

$$(T = \tau, X, Y, Z) \quad \text{on mouth 1 is the same as} \\ (T' = \tau, X' = -X, Y' = Y, Z' = Z) \quad \text{on mouth 2.} \qquad (28)$$

If this is confusing, see Fig. 8 and associated discussion in Ref. 6, where the same construction is described in a slightly different manner.

The structure of the Cauchy horizon $\mathcal{H}_-$ for this spacetime is deduced in the Appendix of Ref. 6. $\mathcal{H}_-$ is generated by null geodesics that peel off of the closed null geodesic $\mathcal{C}$ ($X = T$, $Y = Z = 0$) traveling toward the future. There are caustics in the structure of $\mathcal{H}_-$ on the left side of mouth 1 ($X < -2b$, $Y = Z = 0$) and the right side of mouth 2 ($X' > 2b$, $Y' = Z' = 0$), at which generators cross each other and leave $\mathcal{H}_-$. This accounts for the sharp left-hand corner on $\mathcal{H}_-$ in Fig. 1.

## V. VACUUM POLARIZATION ON THE WORMHOLE'S THROAT

In this section we shall sketch a detailed calculation of the vacuum polarization and its implications arbitrarily close to, but just outside the wormhole's throat/mouths in the spacetime of Fig. 1. We begin in subsection A by calculating the $N$th geodetic interval $\sigma_N$ for rightward-propagating geodesics between our split points $x'$ and $x$ (positive $N$), and from this $\sigma_N$ we deduce the locations, on the throat, of the polarized hypersurfaces $\mathcal{H}_N$ and the Cauchy horizon $\mathcal{H}_-$. In subsection B we compute the $N$th scalarized Van Vleck–Morette determinant $\Delta_N$. In subsection C we combine these and use symmetry considerations to obtain the full regularized Hadamard function, including both leftward geodesic contributions and

rightward ones. In subsection D we compute, from the regularized Hadamard function, the renormalized stress-energy tensor. Finally, in subsection E we compute, from the stress-energy tensor, the total four-momentum carried through the throat, by vacuum fluctuations, in the vicinity of $\mathcal{H}_N$ and in the vicinity of $\mathcal{H}_-$.

Throughout our analysis we restrict ourselves to a wormhole whose radius $b$ is far smaller than the mouths' separation $D$ at the moment the Cauchy horizon reaches mouth 2.

## A. $N$th geodetic interval

Our original computations of the $N$th geodetic interval $\sigma_N$ were carried out by brute force. However, after obtaining the answer, we found the following simpler, but somewhat delicate way to derive the result (delicate in the sense that one has to think hard at several points to be sure the steps taken are correct).

We begin by computing $\sigma_N$ for split points $x'$, $x$ that lie on the $X$ axis and very close to, but just outside mouth 1. Then we shall graft on the effects of a transverse displacement of $x'$ and $x$ from the $X$ axis.

### 1. Points $x'$, $x$ on symmetry axis

When $x'$ and $x$ lie on the $X$ axis (the spacetime's axis of symmetry), the rightward-propagating geodesic $\mathcal{G}_N$ connecting them will lie in the $X$-$T$ plane. Computation of the interval $\sigma_N$ along $\mathcal{G}_N$ then involves only the two spacetime dimensions $X$ and $T$, and it becomes the same as computing $\sigma_N$ in the two-dimensional Misner universe[20] [two-dimensional flat spacetime with the lines $(X = 0, \ T = \tau)$ and $(X = D - \beta\gamma\tau, \ T = D + \gamma\tau)$ identified]. That computation has been carried out by Hiscock and Konkowski[21] in an analysis that has strongly influenced our own work. We shall sketch a slightly altered version of their computation, because a clear understanding of it will be essential to the subsequent steps in our analysis.

The computation is carried out in the covering space of the $T$-$X$ plane of our spacetime (which is the same as the covering space of the Misner universe); see Fig. 5. This covering space depicts successive copies of the region between the right edge of mouth 1 and the left edge of mouth 2 (which both coincide with the wormhole throat). The world lines of the throat/mouth edges are labeled $\mathcal{T}_0, \mathcal{T}_1, \mathcal{T}_2, \ldots$; and the copies are sandwiched between these throat world lines. The covering space's Minkowski coordinates $\tilde{T}$ and $\tilde{X}$ are related to the physical spacetime's Minkowski coordinates $T$, $X$ in copy 0 by

$$\tilde{T} = T - D/(1 - \xi), \quad \tilde{X} = X - D/(1 - \xi) , \qquad (29)$$

where $\xi$ is the inverse of the Doppler blueshift that light acquires when it passes along the $X$ axis and through the wormhole:
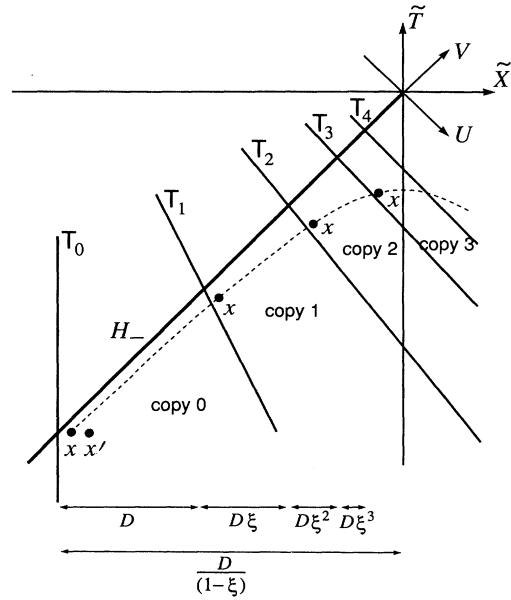


FIG. 5.   Covering space for the $X$-$T$ plane of the wormhole spacetime of Fig. 1.

$$\xi \equiv \left(\frac{1 - \beta}{1 + \beta}\right)^{1/2} . \qquad (30)$$

The Cauchy horizon is at $T = X$ in the physical space and thus also is at $\tilde{T} = \tilde{X}$ in the covering space. Copy $\mathcal{T}_0$ of the throat is at $\tilde{X} = -D/(1 - \xi)$, and copy $\mathcal{T}_n$ is at

$$\left(\tilde{T} + \frac{\xi^n D}{1 - \xi}\right) = \left(\frac{1 + \xi^{2n}}{1 - \xi^{2n}}\right)\left(\tilde{X} + \frac{\xi^n D}{1 - \xi}\right) . \qquad (31)$$

In our discussion we shall find the covering-space null coordinates

$$U \equiv \tilde{X} - \tilde{T}, \quad V \equiv \tfrac{1}{2}(\tilde{X} + \tilde{T}) \qquad (32)$$

more useful than the Minkowski coordinates $(\tilde{T}, \tilde{X})$. The factor $\frac{1}{2}$ in Eq. (32) makes $V$ the same, in copy 0 of the physical spacetime, as spatial distance $X$ along the horizon or along any other $X$-directed null geodesic; and the fact that the covering space has Minkowski geometry guarantees that this $V$ is an affine parameter along these geodesics, not just in copy 0 but throughout the covering space. Our peculiar choice of sign for $U$ makes the geodetic interval take the simple form $\sigma = \Delta U \Delta V$.

The mapping between copy 0 and copy $n$ of the physical spacetime takes a very simple form in the null coordinates: An event $x$ which appears at $U_0(x)$, $V_0(x)$ in copy 0 will appear in copy $n$ at

$$U_n(x) = \xi^{-n} U_0(x), \quad V_n(x) = \xi^n V_0(x) . \qquad (33)$$

These various copies of $x$ all lie on a hyperbola in the covering space (dashed curve in Fig. 5).

The geodesic $\mathcal{G}_N$, with $N$ positive, reaches from copy 0 of $x'$ in the covering space to copy $N$ of $x$; and correspondingly, the $N$th geodetic interval is given by

$$\sigma_N = [V_N(x) - V_0(x')][U_N(x) - U_0(x')] \ . \tag{34}$$

The first factor is huge, and since the two points are very close to the wormhole throat and also close to the Cauchy horizon, it is very nearly the same as the total affine parameter lapse $\Delta V$ along the Cauchy horizon from copy 0 of the throat to copy $N$. We shall call this total affine parameter lapse $\zeta_N$, so

$$V_N(x) - V_0(x') = \zeta_N \ , \tag{35}$$

and from the lengths marked off in Fig. 5, it should be clear that

$$\zeta_N = \sum_{n=0}^{N-1} D\xi^n = \left(\frac{1 - \xi^N}{1 - \xi}\right) D \ . \tag{36}$$

The second factor in the geodetic interval (34) is tiny, and is readily seen from Eqs. (33), (32), and (29) to be given by

$$U_N(x) - U_0(x') = (X - T)\xi^{-N} - (X' - T') \ . \tag{37}$$

Combining Eqs. (34), (35), and (37), we obtain for the geodetic interval

$$\sigma_N = \zeta_N[(X - T)\xi^{-N} - (X' - T')] \ . \tag{38}$$

### 2. Points $x'$, $x$ on wormhole throat

We ultimately, in this section, are interested in split points $x'$, $x$ that lie very close to the wormhole throat and not necessarily on the symmetry axis. As a next step in working our way toward such points, let us put them precisely on the throat, but off the axis.

Displacing $x'$ and $x$ off the symmetry axis and onto the throat affects the geodesic $\mathcal{G}_N$ between them, and correspondingly its geodetic interval $\sigma_N$, in two ways. (i) $\mathcal{G}_N$ acquires some transverse motion, which produces a contribution to $\sigma_N$ that is quadratic in $b$, the wormhole radius. We shall ignore this effect, since the other one is linear in $b$ and thus is far larger. (ii) The points $x$ and $x'$, though on the throat, are displaced in the $X$ direction relative to the throat positions shown in the covering-space diagram, Fig. 5. Specifically, if we denote by

$$\rho \equiv \sqrt{Y^2 + Z^2}, \quad \rho' \equiv \sqrt{Y'^2 + Z'^2} \tag{39}$$

the transverse distance of $x$ and $x'$ from the $X$ axis, then at fixed $T'$ copy 0 of $x'$ (left end of the geodesic $\mathcal{G}_N$) is displaced from the covering-space throat location by an amount

$$\Delta \tilde{X}_0(x') = -b + \sqrt{b^2 - \rho'^2} < 0 \ , \tag{40a}$$

and at fixed $T$ copy $N$ of $x$ (right end of $\mathcal{G}_N$) is displaced from the covering-space throat location by

$$\Delta \tilde{X}_N(x) = \xi^{-N}(b - \sqrt{b^2 - \rho^2}) > 0 \ . \tag{40b}$$

(As we shall see in the next section, at all intermediate throat crossings, $\mathcal{G}_N$ is very nearly on the $X$ axis, $\rho \ll b$; and consequently, we do not need to correct the covering space's descriptions of these crossings.) As a result of the end-point displacements (40a), (40b), the geodetic interval (38) is altered to read [cf. Eq. (34)]

$$\sigma_N = \zeta_N[(b - \sqrt{b^2 - \rho^2} - T)\xi^{-N} - (-b + \sqrt{b^2 - \rho'^2} - T')] \ . \tag{41}$$

From this expression we can read off the location of the $N$th polarized hypersurface $\mathcal{H}_N$ on the inner face (right face of mouth 1 and left face of mouth 2) of the wormhole throat/mouths. If we denote by $\theta$ the polar angle on that inner face,

$$\rho = b \sin\theta, \quad X + b = b \cos\theta \ , \tag{42}$$

and if we collapse the two points $x'$ and $x$ together, then expression (41) becomes

$$\sigma_N(x, x) = \zeta_N[(1 + \xi^{-N})b(1 - \cos\theta) + T(1 - \xi^{-N})] \ .$$

The polarized hypersurface is the location where this geodetic interval vanishes (i.e., where the $N$th geodesic $\mathcal{G}_N$ from $x$ to $x$ is null). It thus is given by the equation

$$T = T_{\mathcal{H}_N}(\theta) \equiv \left(\frac{1 + \xi^N}{1 - \xi^N}\right) b(1 - \cos\theta) \quad \text{for } 0 \le \theta < \pi/2 \ . \tag{43}$$

This equation exhibits the nesting of the polarized hypersurfaces, which we deduced in Sec. II A. On the throat's polar axis $\theta = 0$, all the $\mathcal{H}_N$ occur at the same time, $T = 0$, but away from the polar axis one meets the $\mathcal{H}_N$ one after another as $T$ increases, beginning with arbitrarily large $N$ and ending with $N = 1$.

The Cauchy horizon on the inner face of the throat/mouths is the limit of these $\mathcal{H}_N$ as $N \to \infty$, i.e., it is located at

$$T = T_{\mathcal{H}_-} = \lim_{N \to \infty} T_{\mathcal{H}_N} = b(1 - \cos\theta) \quad \text{for } 0 \le \theta < \pi/2 \ . \tag{44a}$$

The location of the Cauchy horizon on the *outer* face of the throat/mouths can only be understood if one relaxes slightly our demand that the throat be infinitesimally thin (cf. Fig. 10 of Ref. 6). With a tiny but finite throat thickness, one recognizes that on the outer face the Cauchy horizon is generated by null geodesics that get caught on the throat at $(\theta = \pi/2, T = b)$ and then travel along the throat until they reach the outer polar axis, $\theta = \pi$, where they cross each other thereby exiting from the Cauchy horizon. The null-geodesic world lines of these generators are given by

$$T = T_{\mathcal{H}_-}(\theta) = b[1 + (\theta - \pi/2)] \quad \text{for } \pi/2 \le \theta \le \pi \ . \tag{44b}$$

### 3. Points x', x slightly displaced from throat

Now move the points $x'$ and $x$ slightly off the throat in the $X$ direction. If $X'$ and $X$ are their new $X$ coordinates, then their displacements in the physical spacetime from the throat locations assumed in Eq. (41) are $\Delta X = X - (-b + \sqrt{b^2 + \rho^2})$, $\Delta X' = X' - (-b + \sqrt{b^2 + \rho'^2})$. Correspondingly, we must add these $\Delta X$ and $\Delta X'$ to the two terms in parentheses in Eq. (41) [cf. Eq. (38)]. The result is

$$\sigma_N = \zeta_N [(2b - 2\sqrt{b^2 - \rho^2} + X - T)\xi^{-N} - (X' - T')] ,$$

which we shall rewrite in the following form, in order to simplify later notation:

$$\sigma_N = \zeta_N \xi^{-N} \lambda_N(x, x') , \qquad (45)$$

where

$$\lambda_N(x, x') \equiv 2(b - \sqrt{b^2 - \rho^2}) + X - T - (X' - T')\xi^N . \tag{46}$$

Equation (45) is our final expression for the $N$th geodetic interval, with $N > 0$, when the points $x$ and $x'$ are very close to the throat.

### B. Scalarized Van Vleck–Morette determinant

Turn, now, to the scalarized Van Vleck–Morette determinant $\Delta_N$ in this wormhole spacetime. We shall evaluate it using the method of Eq. (24): propagation of an ultra-high-frequency classical scalar wave $\psi$ via elementary geometric optics.

The scalar wave is to be propagated along a null geodesic $\mathcal{C}_{\mathcal{N}}$ that is very nearly the same as the geodesic $\mathcal{G}_N$ which begins at $x'$, travels through the wormhole $N$ times, and ends at $x$. Since $x$ and $x'$ are both close to the Cauchy horizon and close to the inner pole, $\theta = 0$, of the wormhole throat/mouths, a reasonable choice for $\mathcal{C}_{\mathcal{N}}$ is that portion of the Cauchy horizon which reaches from its intersection with copy 0 of the throat, $\mathcal{T}_0$, in the covering space of Fig. 5, to its intersection with copy $N$ of the throat. We use as the affine parameter for this $\mathcal{C}_N$ the covering-space null coordinate $V$, which coincides with proper distance $X$ traveled on the first leg of the geodesic's trip (in copy 0 of Fig. 5). Then the total affine parameter distance traveled is the $\zeta_N$ of Eq. (36) [which is why we used the same notation for it and for the $\zeta_N$ in our discussion of the computation of $\Delta_N$, Eq. (24)].

The amplitude that the wave has at the end of its trip is

$$\psi_N = \frac{1}{D} \left(\frac{b}{2D}\right)^{N-1} . \qquad (47)$$

Here the $1/D$ is the amplitude when the wave first hits mouth 2 (after propagated freely a distance $D$ from its starting point at mouth 1); and each factor of $b/2D$ is the result of defocusing by the wormhole (which acts, in the rest frame of the wormhole, like a lens with focal length $b/2$), followed by propagation over the distance $D \gg b/2$ from mouth 1 to mouth 2. (It is important in these considerations that Doppler shifts have no affect whatsoever on the amplitude of a scalar field.)

The square root of the scalarized Van Vleck–Morette determinant is the ratio of this $\psi_N$ to the amplitude, $1/\zeta_N$, that the wave would have had if there had been no defocusing; cf. Eq. (24):

$$\Delta_N^{1/2} = \left(\frac{\zeta_N}{D}\right) \left(\frac{b}{2D}\right)^{N-1} . \qquad (48)$$

### C. Regularized Hadamard function $G^{(1)}$

In view of expression (45) for $\sigma_N$ and expression (48) for $\Delta_N^{1/2}$, the order-$N$ piece of the regularized Hadamard function (3), for $N > 0$, is

$$\frac{1}{4\pi^2} \frac{\Delta_N^{1/2}}{\sigma_N} = \frac{\xi}{4\pi^2 D} \left(\frac{b\xi}{2D}\right)^{N-1} \frac{1}{\lambda_N(x, x')} , \qquad (49)$$

where $\lambda_N(x, x')$ is given by Eq. (46).

The corresponding piece of $G^{(1)}_{\text{reg}}$ for $N < 0$ can be obtained from this one for $N > 0$ by symmetry considerations: leftward (past-directed) travel from $x'$ to $x$ is equivalent to rightward (future-directed) travel from $x$ to $x'$. Correspondingly, for $N > 0$, $\sigma_{-N}$ and $\Delta_{-N}$ can be obtained from $\sigma_{+N}$ and $\Delta_{+N}$ by simply interchanging the roles of the points $x'$ and $x$. This interchange has no influence on the $\Delta_N$ of Eq. (48), while in the $\sigma_N$ of Eq. (45) it corresponds to interchanging $x'$ and $x$ as arguments of the function $\lambda_N$. Correspondingly, the full regularized Hadamard function, with leftward ($N < 0$) contributions included as well as rightward ($N > 0$) ones, is given by a sum over the contributions (49), augmented by the same sum but with $x'$ and $x$ interchanged in $\lambda_N$:

$$G^{(1)}_{\text{reg}} = \sum_{N=1}^{\infty} \frac{\xi}{4\pi^2 D} \left(\frac{b\xi}{2D}\right)^{N-1} \left(\frac{1}{\lambda_N(x, x')} + \frac{1}{\lambda_N(x', x)}\right) . \tag{50}$$

Here $\lambda_N$ is given by Eq. (46). Notice that this Hadamard function is symmetric under interchange of $x'$ and $x$, as its definition (1) in terms of field operators and its regularization procedure (3) demand.

### D. Renormalized stress-energy tensor $T^{\mu\nu}$

It is straightforward to differentiate the regularized Hadamard function (50) twice and then collapse the points $x'$ and $x$ together and onto mouth 1 of the wormhole, to get the renormalized stress-energy tensor [Eqs. (4)]. The result is

$$T^{\mu\nu} = \frac{-\xi}{6\pi^2 D}\sum_{N=1}^{\infty}\left(\frac{b\xi}{2D}\right)^{N-1}\frac{(1+4\xi^N+\xi^{2N})k^\mu k^\nu + (2+4\xi^N)\tan\theta(k^\mu\hat{\rho}^\nu+\hat{\rho}^\mu k^\nu)+4(\tan^2\theta)\hat{\rho}^\mu\hat{\rho}^\nu}{[b(1-\cos\theta)(1+\xi^N)-T(1-\xi^N)]^3}. \tag{51}$$

Here $\hat{\rho}^\mu$ is the unit transverse vector at the wormhole's mouth 1 (left mouth), and $k^\mu$ is the null vector, with unit spatial length, pointing along the $X$ direction:

$$\hat{\rho} = \frac{\partial}{\partial\rho} = \frac{1}{\sqrt{X^2+Y^2}}\left(Y\frac{\partial}{\partial Y}+Z\frac{\partial}{\partial Z}\right),$$

$$\mathbf{k} = \left(\frac{\partial}{\partial X}+\frac{\partial}{\partial T}\right); \tag{52}$$

$\theta$ is polar angle on the wormhole throat [Eq. (42)], $\xi$ is the inverse Doppler shift produced by the motion of the mouths [Eq. (30)], $b$ is the throat radius, $D$ is the distance between the mouths when the Cauchy horizon arises, and $T$ is Lorentz time at the wormhole's left mouth (mouth 1).

The divergent behavior of this stress-energy tensor as $\theta \to \pi/2$ (i.e., as $\tan\theta \to \infty$) is caused by our idealization of the wormhole throat as vanishingly short. If we were to give the throat a finite thickness $a$, then the $\tan\theta$ factors in Eq. (51) would be cut off at a maximum value of order $b/a$ as $\theta \to \pi/2$.

Note that the stress-energy tensor (52) agrees with the order-of-magnitude estimate (8) derived in Sec. II.

### E. Four-momentum carried by vacuum polarization

The total four-momentum carried by vacuum polarization out of mouth 1 and into mouth 2, up to a time $\Delta T$ before the $N$th polarized hypersurface $\mathcal{H}_N$, is

$$P_N^\mu \equiv \int_{-\infty}^{T\mathcal{H}_N-\Delta T}\int_0^{\pi/2}\int_0^{2\pi}T^{\mu\nu}n_\nu b^2\sin\theta\, d\phi\, d\theta\, dT$$

$$= \frac{-2b}{3\pi}\left(\frac{l_P}{\Delta T}\right)^2\ln\left(\frac{b}{a}\right)\left(\frac{b\xi}{2D}\right)^N\frac{1+2\xi^N}{(1-\xi^N)^3}k^\mu. \tag{53}$$

Here $\mathbf{n} \equiv \cos\theta\partial/\partial X + \sin\theta\hat{\rho}$ is the unit radial vector at mouth 1, and we have integrated only over the inner face of the throat/mouths, $0 \le \theta \le \pi/2$, because, for our arbitrarily short wormhole, the stress-energy tensor should be vanishingly small on the outer face, $\pi/2 \le \theta \le \pi$. The reason is that the geodesics $\mathcal{G}_N$ on the outer face should experience arbitrarily large defocusing and thus have arbitrarily small $\Delta_N^{1/2}$—and thence arbitrarily small $T^{\mu\nu}$; cf. the figures in the Appendix of Ref. 6. The dominant contribution to the $\theta$ integral in Eq. (53) comes from $\theta$ near, but slightly less than $\pi/2$, where the integrand goes like $\tan\theta$, producing the $\ln(b/a)$ term. Here $a$ is the tiny length of the wormhole throat, which provides a $\ln(b/a)$ cutoff on the integral; cf. the discussion in the next to the last paragraph of the preceding section.

Notice that the four-momentum (53) is null and is directed along the $X$ axis, and its time component, the

total energy transfer, is negative. For $\Delta T \sim l_P$, the time component is in accord with the order-of-magnitude estimate in Sec. II, Eq. (15a).

In response to the negative energy transfer, the active gravitational mass of mouth 2 goes down, and that of mouth 1 goes up. In response to the momentum transfer, the two mouths experience an impulsive force toward each other. However, because of the factor $(b/2D)^N$ in the four-momentum transfer, these mass changes and impulsive forces are arbitrarily small, for arbitrarily large $b/D$; and independently of the size of $b/D$ (if our conjecture of a quantum-gravity cutoff at $\Delta T \sim l_P$ is correct) they last for only a time of order the Planck time: In the first few Planck times after the polarized hypersurface, there is an equal and opposite four-momentum transfer that cancels out the earlier mass changes and counteracts the earlier impulsive forces.

The total four-momentum that exits from the inner face of mouth 1 up to a time $\Delta T$ before the Cauchy horizon $\mathcal{H}_-$ is

$$P_-^\mu \equiv \int_{-\infty}^{T\mathcal{H}_- -\Delta T}\int_0^{\pi/2}\int_0^{2\pi}T^{\mu\nu}n_\nu b^2\sin\theta\, d\phi\, d\theta\, dT$$

$$= \frac{-m_P}{6\pi}\frac{l_P}{\Delta T}\sum_{N=1}^{\infty}\left(\frac{b}{2D}\right)^N\left(\frac{1+4\xi^N+\xi^{2N}}{(1-\xi^N)^2}\right)k^\mu. \tag{54}$$

(Here it is justified to keep the terms of all orders $N$, since the dominant contribution for each $N$ comes from very near the closed null geodesic $\mathcal{C}$ to which the polarized hypersurface $\mathcal{H}_N$ is tangent, and thus comes from very near $\mathcal{H}_N$.) Note that if our conjecture of a cutoff at $\Delta T \sim l_P$ is correct, the total four-momentum transfer up to the Cauchy horizon is of order $b/D$ times the Planck mass, $m_P \sim 10^{-5}$ g. If Hawking's conjecture of a cutoff no sooner than $D\Delta T \sim l_P^2$ is correct, the total four-momentum transfer is of order $b$.

### VI. VACUUM POLARIZATION BETWEEN THE WORMHOLE MOUTHS

We now turn from vacuum polarization at the wormhole throat to vacuum polarization in the region between the two mouths. Our calculations here will be patterned after those at the throat. Throughout our analysis we shall assume that (i) the throat size is small compared to the mouth separations, $b \ll D$, (ii) the split points $x'$, $x$ are far from both wormhole mouths, $X \gg b$ and $(D-X) \gg b$, and (iii) the transverse separation of the split points from the $X$ axis is small compared to their distances from the mouths, $\rho \ll X$ and $\rho \ll (D-X)$. In making approximations, we shall regard $X \sim (D-X) \sim D$.

In subsection A we shall derive $\sigma_N$ for rightward-

propagating geodesics, $N > 0$; in subsection B we shall derive $\Delta_N$; in subsection C we shall combine these and invoke symmetry to obtain the regularized Hadamard function $G^{(1)}_{\text{reg}}$; in subsection D we shall derive the renormalized stress-energy tensor $T^{\mu\nu}$; and in subsection E we shall compute the four-momentum carried between the two mouths by vacuum polarization, in the vicinities of the polarized hypersurfaces and the Cauchy horizon.

### A. Nth geodetic interval

As at the throat, so also between the mouths, our original calculations were done by brute force, but we present here a far simpler, *ex post facto* derivation.

For $x'$ and $x$ on the symmetry axis, the $N$th geodetic interval $\sigma_N$ can be derived with ease using covering-space arguments (Fig. 5). As in Sec. V A 1, the result is

$$\sigma_N = \zeta_N \Delta U \tag{55}$$

[cf. Eqs. (34) and (35)], where $\Delta U$ is the tiny covering-space $U$-coordinate length of the geodesic $\mathcal{G}_N$,

$$\Delta U = (X - T)\xi^{-N} - (X' - T') \tag{56}$$

[Eq. (37)], and where the total affine parameter length $\zeta_N$ of $\mathcal{G}_N$ is changed from Eq. (36) because of the new locations of the split points. It is easy to see from Fig. 5 that, with the new longitudinal locations (depicted spatially in Fig. 6),

$$\zeta_N = D - X + \sum_{n=1}^{N-1} D\xi^n + X\xi^N$$

$$= \left(\frac{1 - \xi^N}{1 - \xi}\right) D - (1 - \xi^N)X . \tag{57}$$

As an aid in deducing the effect of moving $x'$ and $x$ off the $X$ axis, we draw in Fig. 6 a spatial diagram of the trajectory of the geodesic $\mathcal{G}_N$ for the illustrative case $N = 3$. The geodesic has four successive legs, labeled 1,2,3,4.

Whenever a ray passes through a strongly diverging lens, in order to keep its outgoing slope less than or of order its ingoing slope, the ray must hit the lens very close to the optic axis: at a transverse distance less than or of order the lens's focal length times the incoming slope. This principle, applied to our wormhole (with its
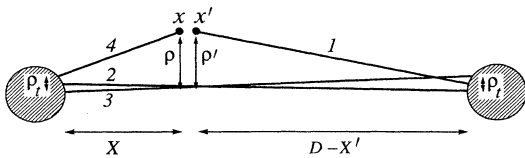
focal length $b/2$ and with the ray slopes of order $\rho/D$ on the first and last legs) implies that all the legs must intersect the wormhole throat in a region near the $X$ axis with transverse size

$$\rho_t \lesssim \rho b/D . \tag{58}$$

This size is tiny compared to the transverse location $\rho$ of the split points. Correspondingly, transverse motion of the geodesic is important only on its first and last legs. These first and last transverse motions increase the $U$ length of the geodesic by

$$\delta \Delta U = \frac{\rho'^2}{2(D - X')} + \frac{\rho^2}{2X}\xi^{-N} . \tag{59}$$

Here the terms $\rho'^2/2(D - X')$ and $\rho^2/2X$ are the increases in the physical lengths of the legs, and the factor $\xi^{-N}$ is the quantity by which physical lengths must be multiplied to get affine lengths $U$ for the last leg; cf. Eq. (33). By adding this $\delta \Delta U$ onto the $U$ length $\Delta U$ of the geodesic $\mathcal{G}_N$ [Eq. (56)] and then combining with Eq. (55), we obtain our final expression for the geodetic interval:

$$\sigma_N = \zeta_N \xi^{-N} \lambda_N(x, x') , \tag{60}$$

where

$$\lambda_N(x, x') = (X - T) - (X' - T')\xi^N + \frac{\rho^2}{2X} + \frac{\rho'^2}{2(D - X')}\xi^N . \tag{61}$$

By setting this expression for $\sigma_N$ to zero and collapsing the points $x'$ and $x$ together, we can read off the locations of the polarized hypersurfaces $\mathcal{H}_N$:

$$T = T_{\mathcal{H}_N} \equiv X + \frac{\rho^2}{2X(D - X)}\left(\frac{D}{1 - \xi^N} - X\right) . \tag{62}$$

As must be so (cf. Sec. II A), these hypersurfaces are all tangent to the geodesic $\mathcal{C}$ ($T = X$, $\rho = 0$) from which the Cauchy horizon springs; and they are nested in order of decreasing $N$. Their shapes in the vicinity of $\mathcal{C}$, to which our analysis is confined, are paraboloidal; cf. Fig. 1.

The Cauchy horizon is the limit of these $\mathcal{H}_N$ as $N \to \infty$:

$$T = T_{\mathcal{H}_-} \equiv X + \frac{\rho^2}{2X} . \tag{63}$$

### B. Scalarized Van Vleck–Morette determinant

Next we compute $\Delta_N^{1/2}$ by the classical-scalar-wave propagation method of Eq. (24). The scalar wave, emitted from the vicinity of the split points $x'$, $x$, arrives at mouth 2 with amplitude $1/(D - X)$. It then experiences $N - 1$ events of defocusing plus propagation over a distance $D$, and thereby is driven down in amplitude by $N - 1$ factors of $b/2D$. The final defocusing and travel back to the vicinity of $x'$, $x$ reduces the amplitude by a factor $b/2X$. The resulting amplitude, multiplied by the total affine parameter distance traveled [the $\zeta_N$ of Eq. (57)] is $\Delta_N^{1/2}$:



FIG. 6. Spatial diagram of the geodesic $\mathcal{G}_3$ when the split points $x'$, $x$ are in the region between the two wormhole mouths.

$$\Delta_N^{1/2} = \frac{\zeta_N D}{X(D-X)} \left(\frac{b}{2D}\right)^N .$$

(64)

## C. Regularized Hadamard function $G^{(1)}$

By combining Eqs. (60) and (64), we obtain for the order-$N$ piece of the regularized Hadamard function, for $N > 0$,

$$\frac{1}{4\pi^2}\frac{\Delta_N^{1/2}}{\sigma_N} = \frac{D}{4\pi^2 X(D-X)}\left(\frac{b\xi}{2D}\right)^N \frac{1}{\lambda_N(x,x')} .$$

(65)

The total, regularized Hadamard function (or, rather, its dominant singular part, which is all that interests us in this paper) is obtained by adding to expression (65) the contribution from the leftward-propagating geodesic

$\mathcal{G}_{-N}$ [obtainable from Eq. (65) by interchanging $x'$ and $x$, cf. Sec. V C], and by then summing over $N$:

$$G^{(1)}_{\text{reg}} = \sum_{N=1}^{\infty} \frac{D}{4\pi^2 X(D-X)}\left(\frac{b\xi}{2D}\right)^N$$
$$\times \left(\frac{1}{\lambda_N(x,x')} + \frac{1}{\lambda_N(x',x)}\right) ,$$

(66)

where $\lambda_N$ is given by Eq. (61).

## D. Renormalized stress-energy tensor $T^{\mu\nu}$

By differentiating the regularized Hadamard function (66) twice and then collapsing the points $x'$, $x$ together [Eqs. (4)], we obtain the following renormalized stress-energy tensor:

$$T^{\mu\nu} = \frac{-Dk^\mu k^\nu}{6\pi^2 X(D-X)}\sum_{N=1}^{\infty}\left(\frac{b\xi}{2D}\right)^N \frac{1 + 4\xi^N + \xi^{2N}}{\{(X-T)(1-\xi^N) + (\rho^2/2X) + [\rho^2/2(D-X)]\xi^N\}^3} .$$

(67)

Here $k^\mu$ is the null vector pointing along the $X$ direction [Eq. (52)], and fractional corrections of order $\rho/X$ and $\rho/(D-X)$ have been ignored. This stress-energy tensor agrees with the order-of-magnitude estimate (8) derived in Sec. II D.

Note that this $T^{\mu\nu}$ has the "double null form" (proportional to $k^\mu k^\nu$) that one normally associates with radiation. Because of the minus sign and the direction of $k^\mu$, just before the $N$th polarized hypersurface it has the form of a beam of negative-energy radiation propagating from mouth 1 to mouth 2; and just after $\mathcal{H}_N$ it resembles a beam of positive-energy radiation from mouth 1 to mouth 2.

The stress-energy tensor does *not*, however, represent real particles. If it did, then its energy would splay out from the vicinity of mouth 1 along straight lines and much of it would escape to future null infinity. By contrast, the energy emerges from mouth 1 and then converges onto mouth 2; cf. the factor $X(D-X)$ in the denominator of Eq. (67). [The directionality $k^\mu k^\nu$ in (67) does not exhibit this expansion followed by convergence because we have computed only the leading-order part of the directionality and have confined ourselves to points far from the mouths. However, one sees the expansion followed by convergence in the throat's stress-energy tensor (51), which also exhibits strong deviations from a radiative-type, double null structure.]

The physical nature of the vacuum polarization, in fact, is much more akin to that of the Casimir vacuum than to that of radiation. To see the connection with the Casimir vacuum, consider a flat spacetime that is closed spatially along one direction by, e.g., identifying $X = 0$ with $X = L$. The vacuum of this spacetime is of the Casimir type, and its nonzero $T^{\mu\nu}$ arises from the periodic boundary conditions on the field $\phi$ imposed by the identification of $X = 0$ with $X = L$. The simplest way to

compute the Hadamard function for this spacetime is by the method of images, which is equivalent to introducing a covering space. The covering space is identical to that of the $X$-$T$ part of our wormhole spacetime (Fig. 5) in the limit $\xi \to 1$ that the boundaries between the copies of the spacetime (the curves labeled $T_N$ in Fig. 5) are all vertical. Tilting the boundaries toward each other has roughly the same effect as switching to the viewpoint of an observer who moves at high speed toward the boundaries. Correspondingly, our $T^{\mu\nu}$ is roughly like that of the Casimir vacuum, viewed by an observer who moves at high speed along the $X$ direction. Our energy density is negative, just as in the Casimir case, but the high effective speed causes the tensorial structure of our $T^{\mu\nu}$ to become nearly radiative.

## E. Four-momentum carried by vacuum polarization

The total four-momentum that the vacuum polarization carries across a plane perpendicular to the $X$ axis, and up to a time $\Delta T$ before the Cauchy horizon, is

$$P_-^\mu \equiv \int_0^\infty \int_{-\infty}^{T_{\mathcal{H}_-} - \Delta T} T^{\mu X}\, dT\, 2\pi\rho\, d\rho$$
$$= \frac{-m_P}{6\pi}\frac{l_P}{\Delta T}\sum_{N=1}^{\infty}\left(\frac{b}{2D}\right)^N \left(\frac{1 + 4\xi^N + \xi^{2N}}{(1-\xi^N)^2}\right) k^\mu .$$

(68)

Notice that this $P^\mu$ is independent of $X$ and is the same as the total four-momentum that flows through the wormhole throat up to one Planck time before the Cauchy horizon. That they are the same is to be expected from energy-momentum conservation, $T^{\mu\nu}_{;\nu} = 0$, plus the fact that, on the part of the hypersurface $T = T_{\mathcal{H}_-} - \Delta T$ where $T^{\mu\nu}$ is very large, it is very nearly parallel to the hypersurface.

It is interesting to compute the total four-momentum transferred *per unit area* across a plane perpendicular to the $X$ axis, at times up to one Planck time before $\mathcal{H}_N$, the $N$th polarized hypersurface:

$$\left(\frac{dP^\mu}{dA}\right)_N \equiv \int_{-\infty}^{t_{\mathcal{H}_N} - l_P} T^{\mu X} dT$$

$$= \frac{-D}{12\pi^2 X(D-X)} \left(\frac{b\xi}{2D}\right)^N$$

$$\times \left(\frac{1 + 4\xi^N + \xi^{2N}}{(1-\xi^N)^3}\right) k^\mu . \qquad (69)$$

Notice the following properties of this four-momentum per unit area: (i) It is independent of transverse location $\rho$ in the regime $\rho \ll D$ to which our analysis is constrained; (ii) it is independent of Planck's constant; (iii) since $N \geq 1$, it is $\lesssim b/D^2$, and thus becomes arbitrarily small when $b/D$ gets arbitrarily large.

## VII. CONCLUSIONS

In this paper we have computed the details of the divergent vacuum polarization for a massless scalar field in spacetimes with closed timelike curves. While we are quite confident of our computations, there are two ways in which we might have erred.

(i) Our computations rely on the assumption that the quantum field theory of a massless scalar field can be formulated in the standard manner, in terms of the field's modes, in wormhole spacetimes with closed timelike curves; see Sec. II B. We see no obvious way that this can fail, but we have not explored all the nooks and crannies of the quantum field theory to be certain.

(ii) Our derivation of the regularized Hadamard function, Eq. (20), might be flawed. For example, our derivation relies on a tacit assumption that the wormhole spacetimes are *benign*[22] for a classical, massless scalar field. If this is not so, then we cannot pose initial data in tiny neighborhoods in the region with CTC's and evolve those data forward in local time in the manner that underlies two pieces of our derivation: (a) the wave-packet modes used to derive the singular part (17) of the Hadamard function, $G^{(1)} = 1/4\pi^2\sigma$, and (b) the propagation of that singular part to get our multiple-geodesic, Hadamard normal form (20) of $G^{(1)}$. To shore up confidence in (or

invalidate) our $G^{(1)}$, one might try to tie it to past null infinity, from which the posing and evolution of initial data are known to be well behaved.[7] For example, one might do so using a variant of the Ford-Parker formalism.[23]

We have argued in this paper (and Hawking has argued to the contrary) that quantum gravity cuts off the vacuum-polarization divergence near the Cauchy horizon when it is still far too small to prevent the creation of closed timelike curves. If we are correct, then how might the laws of physics protect the universe from CTC's—or do they?

In view of everything that we and others have learned about this issue during the past several years,[1-4,6,7,11,8,9,16,22,24] there seems to be only one other likely method, besides divergent vacuum polarization, for protecting against CTC's: The laws of physics might completely forbid the existence of traversable wormholes, e.g., by enforcing the averaged weak energy condition on null geodesics that thread a wormhole,[2,3,6] or by preventing wormholes from forming dynamically.[2] Whether this is the case is far from obvious.

Alternatively, it just might be that the fundamental laws of physics find closed timelike curves acceptable. Hints that this might be so have been seen recently in the surprisingly good behavior of the Cauchy problem for evolution of physical systems in wormhole spacetimes with closed timelike curves.[6,7,11,24]

## ACKNOWLEDGMENTS

*Present address: Ewha Womans University, 11-1, Daehyun-Dong, Seodaemun-Gu, Seoul, Korea.
[1] M.S. Morris and K.S. Thorne, Am. J. Phys. **56**, 395 (1988).
[2] M.S. Morris, K.S. Thorne, and U. Yurtsever, Phys. Rev. Lett. **61**, 1446 (1988).
[3] G. Klinkhammer, Phys. Rev. D **43**, 2542 (1991); U. Yurtsever, Class. Quantum Grav. Lett. **7**, L251 (1990); R.M. Wald and U. Yurtsever, Phys. Rev. D (to be published); C. Cutler (unpublished).
[4] I.D. Novikov, Zh. Eksp. Teor. Fiz. **95**, 769 (1989) [Sov. Phys. JETP **68**, 439 (1989)]; V.P. Frolov and I.D. Novikov,

Phys. Rev. D **42**, 1057 (1990).
[5] S.W. Hawking and G.F.R. Ellis, *The Large Scale Structure of Space Time* (Cambridge University Press, Cambridge, England, 1973), Proposition 6.5.3.
[6] J. Friedman, M.S. Morris, I.D. Novikov, F. Echeverria, G. Klinkhammer, K.S. Thorne, and U. Yurtsever, Phys. Rev. D **42**, 1915 (1990).
[7] J. Friedman and M.S. Morris, Phys. Rev. Lett. **66**, 401 (1991); and (in preparation).
[8] Independent unpublished work by the authors of this paper, by V.P. Frolov, by N. N. Gnedin, and by D. A. Kompaneets.

[9]V.P. Frolov, this issue, Phys. Rev. D **43**, 3878 (1991).

[10]For a review and extensive references to the literature, see V.M. Mostepanenko and N.N. Trunov, Usp. Fiz. Nauk **156**, 385 (1988) [Sov. Phys. Usp. **31**, 965 (1988)]. For interacting fields, see, e.g., B.S. Kay, in *Proceedings of the Second Marcel Grossmann Meeting on the Recent Developments of General Relativity*, Trieste, Italy, edited by R. Ruffini (North-Holland, Amsterdam, 1982), p. 127; B.S. Kay, Phys. Rev. D **20**, 3052 (1979). For supersymmetric field theories, see, e.g., Y. Igarashi and T. Nonoyama, Prog. Theor. Phys. **77**, 427 (1987). In the case of a massless scalar field (this paper), switching from conformal coupling to some other curvature coupling leaves unchanged those parts of $G^{(1)}_{\text{reg}}$ that contribute to the dominant divergence of $T_{\mu\nu}$ (see Ref. 18), and in $\mathcal{D}_{\mu\nu}$ [Eq. (4b)], it changes only the numerical coefficients in front of the three terms. As a result, aside from factors of order unity, the dominant divergence of $T_{\mu\nu}$ is independent of the choice of curvature coupling; it always has the form (8).

[11]F. Echeverria, G. Klinkhammer, and K.S. Thorne (in preparation); G. Klinkhammer and K.S. Thorne (in preparation).

[12]J.A. Wheeler, *Geometrodynamics* (Academic, New York, 1962).

[13]S.W. Hawking, presented at a seminar, Cambridge, England, 1990; and (in preparation).

[14]C.W. Misner, K.S. Thorne, and J.A. Wheeler, *Gravitation* (Freeman, San Francisco, 1973); cited in text as MTW.

[15]See, e.g., N.D. Birrell and P.C. Davies, *Quantum Fields in Curved Space* (Cambridge University Press, Cambridge, England, 1982).

[16]V.P. Frolov and I.D. Novikov (in preparation).

[17]R.L. Forward, Phys. Rev. D **26**, 735 (1982).

[18]See, e.g., Sec. 2 of B.S. DeWitt and R.W. Brehme, Ann. Phys. (N.Y.) **9**, 220 (1960). This reference treats the minimally coupled scalar field [no factor $\frac{1}{6}R$ in the wave equation (2)], but its analysis is easily extended to the conformally coupled case. When one does so, the resulting Hadamard normal forms of the Hadamard function [Eqs. (5) and (18)–(21)] and of the propagator [Eq. (23)] are unchanged, the functions $\sigma$ and $\Delta$ are unchanged, but the functions $v$ and $w$ (which are irrelevant for this paper) are altered.

[19]J.A. Wheeler, Ann. Phys. (N.Y.) **2**, 604 (1957); B. S. DeWitt, in *Gravitation: An Introduction to Current Research*, edited by L. Witten (Wiley, New York, 1962), p. 266 and especially Secs. 8–8.5.

[20]C.W. Misner, in *Relativity Theory and Astrophysics I: Relativity and Cosmology*, edited by J. Ehlers (American Mathematical Society, Providence, 1967), p. 160; see also Sec. 5.8 of Ref. 5.

[21]W.A. Hiscock and D.A. Konkowski, Phys. Rev. D **26**, 1225 (1982).

[22]For the formulation of the concept of benignness and strong evidence that wormhole spacetimes with CTC's are, in fact, benign for a massless scalar field, see U. Yurtsever, J. Math. Phys. **31**, 3064 (1990); also Ref. 6.

[23]L.H. Ford and L. Parker, Phys. Rev. D **17**, 1485 (1978).

[24]I.D. Novikov (unpublished); I.D. Novikov and V. Petrova (in progress).